Journal of Alloys and Compounds 901 (2022) 163474

Contents lists available at ScienceDirect

Journal of Alloys and Compounds

journal homepage: www.elsevier.com/locate/jalcom

Ionic conductivity in complex metal hydride-based nanocomposite materials: The impact of nanostructuring and nanocomposite formation

Laura M. de Kort, Valerio Gulino, Petra E. de Jongh, Peter Ngene*

Materials Chemistry and Catalysis, Debye Institute for Nanomaterials Science, Utrecht University, Universiteitsweg 99, 3584CG Utrecht, the Netherlands

ARTICLE INFO

Article history:
Received 19 September 2021
Received in revised form 22 December 2021
Accepted 25 December 2021
Available online 31 December 2021

Keywords:
Batteries
Solid electrolytes
Metal hydrides
Nanocomposites
Nanostructuring
Interface engineering

ABSTRACT

Complex metal hydrides have recently gained interest as solid electrolytes for all-solid-state batteries due to their light weight, easy deformability, and fast ion mobility at elevated temperatures. However, increasing their low conductivity at room temperature is a prerequisite for application. In this review, two strategies to enhance room temperature conductivity in complex metal hydrides, nanostructuring and nanocomposite formation, are highlighted. First, the recent achievements in nanostructured complex metal hydride-based ion conductors and complex metal hydride/metal oxide nanocomposite ion conductors are summarized, and the trends and challenges in their preparation are discussed. Then, the reported all-solid-state batteries based on complex metal hydride nanocomposite electrolytes are highlighted. Finally, future research directions and perspectives are proposed, both for the preparation of improved metal hydride ion conductors, as well as metal hydride-based all-solid-state batteries.

1. Introduction

The desire to reduce our carbon footprint has led to an ongoing search for efficient energy storage devices. Effective energy storage would enable us to deal with the intermittent nature of most renewable energy sources and, thereby, use their energy output efficiently [1–3]. Techniques based on hydro, mechanical, thermal, chemical, and electrochemical systems are being considered for large scale energy storage. Amongst these storage options, electrochemical energy storage, especially in rechargeable batteries, is quite appealing. In fact, lithium-ion batteries are currently one of the most widely used energy storage systems, with applications ranging from mobile devices to electric vehicles. However, their implementation for the storage of renewable electricity at large scales is hindered by some challenges. These include their limited energy density, safety concerns inherent to their flammable organic liquid electrolytes, as well as the rising cost of the battery components, e.g. Li and Co [3–5]. Consequently, much research effort is directed towards the development of new batteries beyond current lithium-ion technology.

The main goals of current research in the battery field are to increase safety and energy density, while reducing the manufacturing cost. The first two goals could be reached by employing inorganic or polymeric solids as the ion-conducting electrolytes (instead of the conventional electrolytes based on lithium salts dissolved in organic solvents), resulting in the so-called all-solid-state (ASS) battery [6–8]. Solid-state electrolytes (SSEs) are often safer than the volatile and combustible liquid electrolytes, and in many cases they are compatible with high capacity electrodes. This means that the development of all-solid-state batteries can potentially lead to safer batteries that store more energy.

Solid-state electrolytes with good ionic conductivity at ambient temperature (~10^{-3} S cm^{-1}) as well as good electrochemical stability are crucial for the implementation of ASS batteries. In recent years, different classes of solid ion conductors have been proposed, each with their own advantages and disadvantages [7–13]. For example, sulfide-type SSEs display excellent ionic conductivity at ambient temperature, but their chemical stability is poor [14,15]. Oxide-based electrolytes, on the other hand, have a higher (electro)chemical stability, but their manufacturing process is expensive and their poor interfacial contact with electrode remains a concern [16–18]. While research has been largely focused on oxide- and sulfide-type SSEs, complex metal hydrides have recently emerged as interesting alternative.

Compared to oxide- and sulfide-type ion conductors, complex metal hydrides display several useful properties that could be beneficial for ASS batteries. Research on metal hydride-based solid electrolytes was initiated by the discovery of unexpectedly fast Li-ion mobility in lithium borohydride. A few years ago, researchers from Orimo's group observed high lithium-ion mobility (10^{-3} S cm^{-1}) after a reversible polymorphic transition from orthorhombic to hexagonal phase at 110 °C [19]. Similar behaviour was later found in many other complex hydrides as well, such as $Li_2B_{12}H_{12}$ and $NaCB_9H_{10}$ [20–22]. In

* Corresponding author.
E-mail address: P.Ngene@uu.nl (P. Ngene).

https://doi.org/10.1016/j.jallcom.2021.163474

addition to the high ionic mobility above their polymorphic transition temperature, they possess other interesting properties that make them attractive for application in ASS batteries. Especially their low weight, combined with a generally high electrochemical stability (up to 3 V versus Li/Li^+) and the ability to form a good interface with electrode materials, distinguish them from most other solid-state ion conductors [23–28].

While a high electrochemical stability and a good interfacial contact with electrodes are essential, the ionic conductivity of a solid-state ion conductor should also be at least 10^{-3} S cm^{-1} at room temperature to be successfully employed in an all-solid-state battery. Unfortunately, most metal hydride ion conductors exhibit moderate room temperature ionic conductivity ($< < 10^{-3}$ S cm^{-1}). Thus, the development of strategies that enhance conductivity in complex hydrides at ambient temperature is of major importance. The main strategies that have been explored include ionic substitution, nanostructuring, and nanocomposite formation. The most commonly reported method, partial ionic substitution, is based on partial replacement of the cations or complex hydride anions with other ions of slightly different size or electronegativity, (e.g. K^+, Ca^{2+} or I^-, Br^-) [29–34]. A homogenous solid solution is formed, which either stabilizes the high-temperature, highly conductive polymorph of the hydride at RT or leads to the formation of double-anion compounds with different crystallographic structure and enhanced ionic conductivity at RT.

Nanostructuring and nanocomposite formation are less common approaches to enhance room temperature conductivity in metal hydrides. Nevertheless, these synthetic approaches are very interesting. With nanostructuring, the crystallite size of the starting material is reduced via high-energy ball milling, thereby reducing the crystalline grain size and introducing defects and structural disorder. Due to the introduction of defects and structural disorder, nanocrystalline ceramics often show an enhanced ion diffusivity compared to their microcrystalline counterparts [35]. While this technique was initially investigated for lithium oxides, such as $LiNbO_3$, it has recently been shown to greatly enhance the conductivity of metal hydride-based solid electrolytes as well [36,37].

Alternatively, the ionic conductivity can be enhanced by intimately mixing the metal hydride with a high surface area non-conducting oxide scaffold, thereby forming a nanocomposite electrolyte [38,39]. In this review, we will refer to this approach as nanocomposite formation or interface engineering. Note that in this method at least two components are combined, as opposed to nanostructuring which involves one component. Intimate contact between the two components is often achieved with high-energy ball milling or via melt infiltration. While this method was originally used to improve hydrogen sorption properties of metal hydrides, in 1973 the pioneering work by Liang et al. on a mixture of LiI and fine inert Al_2O_3 particles demonstrated that nanocomposite formation can lead to enhanced ion mobility in solid ion conductors as well [40]. The introduction of oxides in ion conductors can have different effects, which have recently been extensively reviewed by Zou et al. [38] In short, nanocomposite formation can lead to the stabilization of a nanostructured superionic phase or high-temperature conductive polymorph at ambient temperature, and/or the formation of a conductive interface layer, such as a space charge region or a tertiary compound resulting from reactions at the interface. Notably, in nanocomposites, the advantageous effects of nanostructuring are combined with the benefits of interface interactions between the metal hydride and the oxide scaffold.

Several excellent reviews on metal hydrides for energy purposes have been published, for example by Bannenberg [41], de Jongh [42] and Duchêne [27]. However, the potential of nanostructuring and nanocomposite formation as methods to enhance ionic conductivity in metal hydrides has not been specifically reviewed. Therefore, this review will highlight the design and fabrication of nanostructured and nanocomposite metal hydride-based electrolytes for ASS batteries. Firstly, the mechanisms for ionic conduction in (pristine) complex metal hydrides are described. Thereafter, the latest advances and achievements in metal hydride nanocomposite electrolytes are reviewed, with emphasis on lithium- and sodium conducting compounds, in particular lithium borohydride, which is one of the most investigated metal hydrides in the research field. Following, the application of metal hydride nanocomposite electrolytes in all-solid-state batteries is discussed. Finally, the current trends and challenges of metal hydride nanocomposites are summarized, and future research directions and perspectives are proposed.

2. Ionic conductivity in metal hydrides

Complex metal hydrides are a subclass of metal hydrides. They are solids with an ionic lattice composed of metal cations, and complex anions in which the hydrogen is covalently bound to an atom, such as in BH_4^-, AlH_6^{3-} and $B_{12}H_{12}^{2-}$. This class of materials, commonly known for their application as reducing agents in organic synthesis, has recently shown great potential in various energy-related applications. For a complete overview of their possible applications, the reader is kindly referred to general reviews on metal hydrides as energy materials by Bannenberg et al., Mohtadi et al. and Hirsher et al. [41,43,44] Initially, complex hydrides were proposed as reversible hydrogen storage materials due to their ability to reversibly store large amounts of hydrogen under moderate conditions [45,46]. Later, the high reversible heat accompanying hydrogenation and dehydrogenation, sparked research in the use of metal hydrides for thermal energy storage [47]. Over the past few years, new discoveries of useful metal hydride properties revealed even more possible applications, one of which is the application of metal hydrides as solid-state ion conductors.

2.1. Fast ionic mobility in $LiBH_4$

The consideration of complex hydrides as solid-state electrolytes was driven by the discovery of unexpectedly fast Li-ion mobility in lithium borohydride. At room temperature, $LiBH_4$ has a low ionic conductivity (10^{-8} S cm^{-1} at 30 °C), but a remarkable increase in conductivity is observed at higher temperatures (10^{-3} S cm^{-1} at 120 °C) [48]. This behaviour is caused by a reversible polymorphic transition from the orthorhombic phase to the hexagonal phase at 109 °C, as schematically depicted in Fig. 1 [19]. The Nyquist plots obtained by Electrochemical Impedance spectroscopy show only a single arc in both the low temperature and high temperature polymorph, which indicates a single diffusion mechanism and limited response from grain boundaries [49]. Matsuo et al. were the first to confirm that the increased conductivity is related to fast Li-ion mobility in the hexagonal polymorph using ^7Li NMR measurements [19]. In the orthorhombic polymorph, NMR spectra show broad and small peaks, whereas in the high-temperature polymorph each spectrum displays sharp and narrow peaks. This decrease in linewidth confirmed that the high conductivity in hexagonal $LiBH_4$ is caused by fast Li-ion mobility [19].

To understand the origin of the fast lithium-ion mobility, the conduction mechanism in $LiBH_4$ has been investigated. In the high-temperature hexagonal phase, the Li-ions are arranged in layers in the hexagonal plane with nearly equivalent Li sites [50]. In this structure all Li^+ sites are filled and, consequently, the ionic conduction likely occurs via Frenkel-pair defects, i.e., Li^+ vacancies combined with interstitial Li^+ sites [49–51]. It has been proposed that the movement of interstitial Li^+ ions in $LiBH_4$ is accommodated by the rotation of neighbouring BH_4^--units, the so-called paddle-wheel mechanism [49,52]. In this way, the interstitial Li^+-ions can easily jump from one interstitial site to the next. Interestingly, the

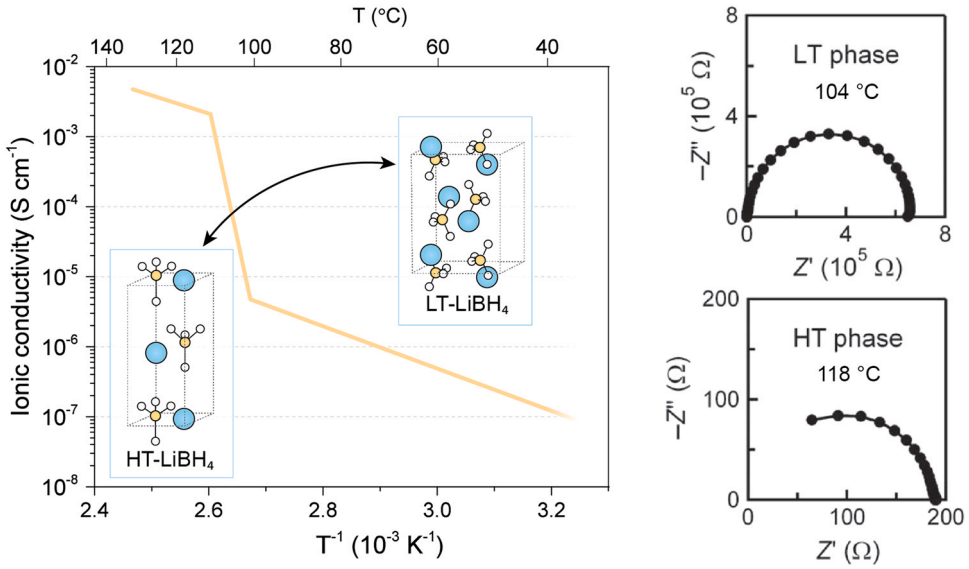

Fig. 1. Arrhenius plot of the conductivity of $LiBH_4$, including a schematic representation of the phase transition from orthorhombic $LiBH_4$ (LT) to hexagonal $LiBH_4$ (HT) and the Nyquist plots obtained for the respective phases[49].

diffusion energy barrier of Li interstitials in *o*-$LiBH_4$ and *h*-$LiBH_4$ is similar, which means that the improvement in conductivity in *h*-$LiBH_4$ cannot be explained by changes in energy barrier for ion migration. On the other hand, the formation energy of defects in the hexagonal structure is substantially lower than in the orthorhombic phase [52,53]. This results in a higher density of defect sites, hence, the higher ion mobility in *h*-$LiBH_4$ likely originates from the lower defect formation energy [53].

2.2. Ionic mobility in borohydrides, alanates and amines

Besides $LiBH_4$, several other complex metal hydrides possess interesting properties which also make them interesting candidates for application in all-solid-state batteries. Most metal hydrides have a low density, are easily deformed and are chemically compatible with metallic lithium or sodium anodes or they form a stable conductive interface, all of which are useful properties for solid-state electrolytes [28,54]. Therefore, the ionic conductivity of several other metal hydrides has been investigated as well.

Most of the initial research was focussed on metal hydrides similar to $LiBH_4$, including $LiAlH_4$, Li_3AlH_6, $LiNH_2$ and Li_2NH, as well as their Na-based counterparts, $NaBH_4$, $NaAlH_4$ and Na_3AlH_6. Unfortunately, most of these metal hydrides show low ionic conductivities at room temperature ($< 10^{-9}$ S cm^{-1}) and none of them undergoes a polymorphic transition that results in an increased Li^+ or Na^+ ion mobility [55–62]. The highest conductivities are observed for Li_3AlH_6, Na_3AlH_6 and Li_2NH, with conductivities of, respectively, $1.4 \cdot 10^{-7}$ S cm^{-1}, $6.4 \cdot 10^{-7}$ S cm^{-1} and $2.5 \cdot 10^{-4}$ S cm^{-1}. Note that Li_2NH was one of the first complex hydrides investigated as possible ion conductor, already reported by Boukamp et al. in 1979 [58]. However, as a result of the relatively low electrochemical stability, the interest in Li_2NH decreased quickly. Due to the discovery of fast ionic conductivity in $LiBH_4$, interest in this compound resurfaced and it has been investigated in more detail recently [60–62]. Similar to $LiBH_4$, it has been reported that anion dynamics and a low defect formation energy are key to achieving high ionic conductivity in the Li-N-H system [62].

In addition to solid electrolytes based on monovalent cations (e.g. Li^+, Na^+), metal hydride with multivalent ion transport such as $Mg(BH_4)_2$ and $Ca(BH_4)_2$ have also been gaining attention lately. Unfortunately, first principles studies on a variety of complex metal hydrides by Lu et al. indicated slow ion transport for divalent species [28]. For instance, pristine magnesium borohydride displays a low ionic conductivity of 10^{-12} S cm^{-1} at RT. Remarkably, with specific modifications, which will be discussed in Section 3.2.4, it is possible to increase the conductivity by over 8 orders of magnitude [63].

2.3. Ionic conductivity in closo-borates and closo-carborates

Recently, a novel series of metal hydride solid-state ion conductors has been introduced based on *closo*-borate and *closo*-carborate cluster anions, e.g. $[B_{12}H_{12}]^{2-}$ and $[CB_9H_{10}]^-$, depicted schematically in Fig. 2a [20,21,64–71]. This class of materials consists of a variety of geometrically similar (car)borate anions, which offers a toolkit of solid-state metal hydride-based compounds with great potential as solid electrolytes. Most *closo*-borates and *closo*-carborates undergo polymorphic transitions from ordered to disordered phases by heating to high temperatures (e.g., 315 °C for $Li_2B_{12}H_{12}$, 106 °C for $NaCB_{11}H_{12}$). Akin to $LiBH_4$, these order-disorder polymorphic transitions are accompanied by a fast reorientational motion of the cage-like cluster anions (the paddle wheel mechanism) and a remarkable increase in ionic conductivity. Recent ab initio molecular dynamics calculations strongly suggest that the fast cation mobility observed in *closo*-(car)borates is closely linked to the motion of the complex hydride anions [72–74]. For example, in $Na_2B_{10}H_{10}$, the reorientation and disorder of the $B_{10}H_{10}^{2-}$ anion facilitates Na^+ hopping to octahedral sites, which links to the tetrahedral sites to form a connected network for fast ion diffusion [72]. The conductivities of $LiBH_4$, $Na_2B_{10}H_{10}$, $Na_2B_{12}H_{12}$, and $LiCB_9H_{10}$ are presented in Fig. 2b [21,65,75]. Just above their polymorphic transition temperature (T_{trans}) both Li^+ and Na^+-*closo*-borate-based ion conductors exhibit conductivities over 0.01 S cm^{-1}. In fact, at temperatures above T_{trans}, the ionic conductivities of some *closo*-(car)borate compounds are comparable to those of state-of-the-art solid-state ion conductors, such as $Li_xLa_xTiO_2$ (10^{-3} S cm^{-1} at 30 °C) and sulfide glass-ceramics (2 ▯ 10^{-2} S cm^{-1} at 30 °C) [13,15,18].

Although the large-scale application of *closo*-(car)borates is presently impeded by the complex, low-yield synthetic pathways, recent studies have shown that it is possible to synthesize different *closo*-(car)borates, e.g. $NaCB_{11}H_{12}$ and $Na_2B_{12}H_{12}$, in a more simple way [76–78]. For example, Berger et al. recently demonstrated a solution-based method to obtain $Me_3NH[CB_{11}H_{12}]$ in which the approximate reagents cost per gram product was reduced from approximately $70 (in other published works) to $13.44 [78]. This

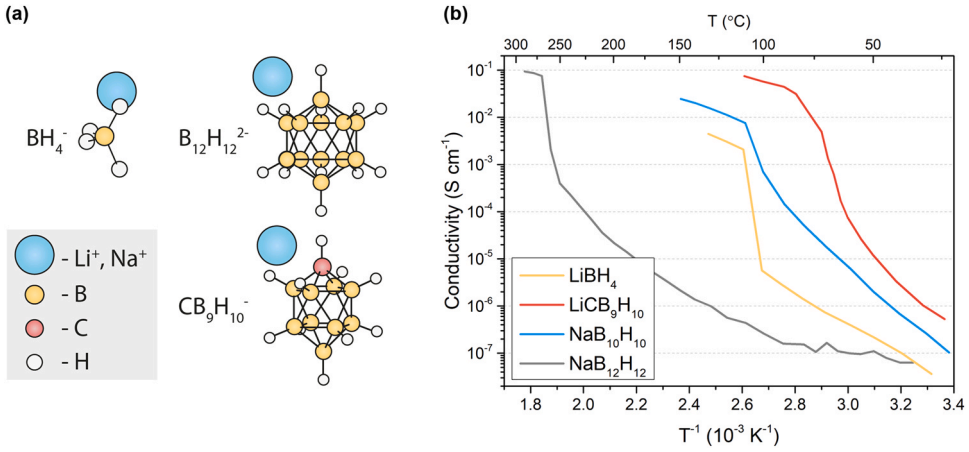

Fig. 2. (a) Schematic representation of Li^+- and Na^+-borohydride, *closo*-borate and *closo*-carborate compounds. (b) Arrhenius plot of the conductivity of different metal hydride compounds. Copyright 2016 Wiley [21], Copyright 2014 Royal Society of Chemistry [65] and Copyright 2014 Wiley [75].
Graphs are adapted with permission from ref [21,65,75].

study illustrates that it might be possible to develop less expensive production processes for *closo*-(car)borates. On the other hand, the costs and safety of the solvents (e.g. DME or THF) used in the proposed synthesis method were not taken into account. For the development of large-scale synthesis routes for *closo*-(car)borates a thorough and critical analysis of the costs and safety of all used chemicals and processing will be necessary.

It is clear that these metal hydrides demonstrate high ionic conductivities above their polymorphic transition temperature, making them promising candidates for next-generation batteries. However, for application in all-solid-state batteries, conductivities of at least 10^{-3} S cm^{-1} at 25 °C are required. The room temperature ion conductivity of most metal hydrides is not yet sufficient and remains inferior to other SSEs [13]. For example, the room temperature Li-ion conductivities for sulfide-based electrolytes are in the order of 10^{-2} S cm^{-1}, which is orders of magnitude higher than the room temperature conductivity of most metal hydride-based solid electrolytes. Consequently, a main challenge for the development of metal hydride electrolytes is to extend their high ionic mobilities to room temperature.

3. Enhanced room temperature conductivity in metal hydrides

Over the past few years different strategies to improve room temperature conductivities in metal hydride-based ion conductors have been explored. These strategies can be classified into three categories, i.e., partial ionic substitution, nanostructuring and nanocomposite formation (or interface engineering), which are schematically depicted in Fig. 3. The most common method, partial ionic substitution, is based on replacing part of the metal hydride anions with other anions. As a result, either a homogenous solid solution is formed, in which the highly conductive polymorph is stabilized at lower temperatures, or a double-anion compound is formed with another crystallographic structure (and possibly enhanced conductivity) [30,79]. For example, ionic substitution of BH_4^- (r_{BH4-} = 2.03 Å) in pristine $LiBH_4$ with either I^- (r_{I-} = 2.20 Å) or Br^- (r_{Br-} = 1.96 Å) leads to stabilization of conductive hexagonal $LiBH_4$ (Fig. 3a). It has been observed that this method only works within the appropriate solubility limits (h-$Li(BH_4)_{1-x}(I)_x$ is only stable in the range $0.18 \le x \le 0.50$ [80]), and with substituting anions of the appropriate size (Cl^-substitution (r_{Cl-} = 1.81 Å) in $LiBH_4$ does not result in stabilization of h-$Li(BH_4)_{1-x}(Cl)_x$ [29]). Over the past years several notable solid solution or double-anion (and even triple-anion) compounds have been developed, including $Li(BH_4)_{1-x}(Br)_x$ [81], $Li(BH_4)_{1-x-y}(Br)_x(Cl)_y$ [82], $Li(BH_4)_{1-x}(NH_2)_x$ [79], $(LiCB_9H_{10})_{0.7}(LiCB_{11}H_{12})_{03}$ [83]., $Na_4(CB_{11}H_{12})_2(B_{12}H_{12})$ [84] and $Na_4(B_{12}H_{12})$-$(B_{10}H_{10})$ [24]. As several review articles have been published on this topic, we won't elaborate further on this specific strategy in this review [27,34,49].

Nanostructuring and nanocomposite formation are less widely applied strategies to enhance conductivity in metal hydride-based ion conductors. Nonetheless, it has been established that these methods can significantly improve ionic mobility in solid-state electrolytes. In the former method, nanostructuring, the metal hydride is mechanochemically activated by high-energy ball milling of the coarse-grained starting material for several minutes up to tens of hours. In general, this process reduces the grain size of the starting material to about 5–50 nm, while introducing defects and structural disorder (Fig. 3b). These nanostructured grains typically consists of two regions, including nanometer-sized crystallites separated by a large volume fraction of grain boundaries or interfacial regions [85,86]. The impact of the milling process on the ion mobility is rather complex and not well understood. In fact, while the formation of defects and grain boundaries can be detrimental for long range ionic transport in some fast ion conductors, poor ionic conductors that largely depend on defect sites could benefit from defect rich grain boundaries that enhance their ionic conductivity. In both cases, nanostructuring clearly alters the ion dynamics in the ionic conductors. First reports on the application of this strategy focussed on the improvement of ionic conductivity in lithium oxides, such as $LiNbO_3$ and $LiTaO_3$ [35,85,87,88]. Recently, the method has also been applied to several metal hydrides, e.g. $LiBH_4$ and $LiAlH_4$, and *closo*-(car)borate compounds, including $Li_2B_{12}H_{12}$ and $NaCB_{11}H_{12}$ [36,37,89–92].

Nanocomposite formation also involves nanostructuring, but in this case the solid electrolyte compound is additionally mixed with a high surface area non-conducting oxide scaffold, such as SiO_2 or Al_2O_3, thereby forming a nanocomposite (Fig. 3c). Close contact between the two components is achieved by high-energy ball milling of the metal hydride with the oxide scaffold or via nanoconfinement of the metal hydride in the nanopores of the oxide by melt infiltration. In 1973 Liang et al. were the first to report on the ionic conductivity of composite solid electrolytes [40]. They showed that combining LiI with Al_2O_3 increased the ion conductivity from 10^{-7} S cm^{-1} to 10^{-5} S cm^{-1}. Since then, this method has been applied to several different ion conductors, including AgI, $LiNO_3$ and, more recently, $LiBH_4$ [93–95].

The enhancement in ionic conductivity upon introduction of the non-conducting scaffold can be attributed to several effects. A short overview of the main phenomena will be discussed here and for a more detailed description the reader is referred to a recent work by Zou et al. [38] Generally, multiple diffusion processes are involved in

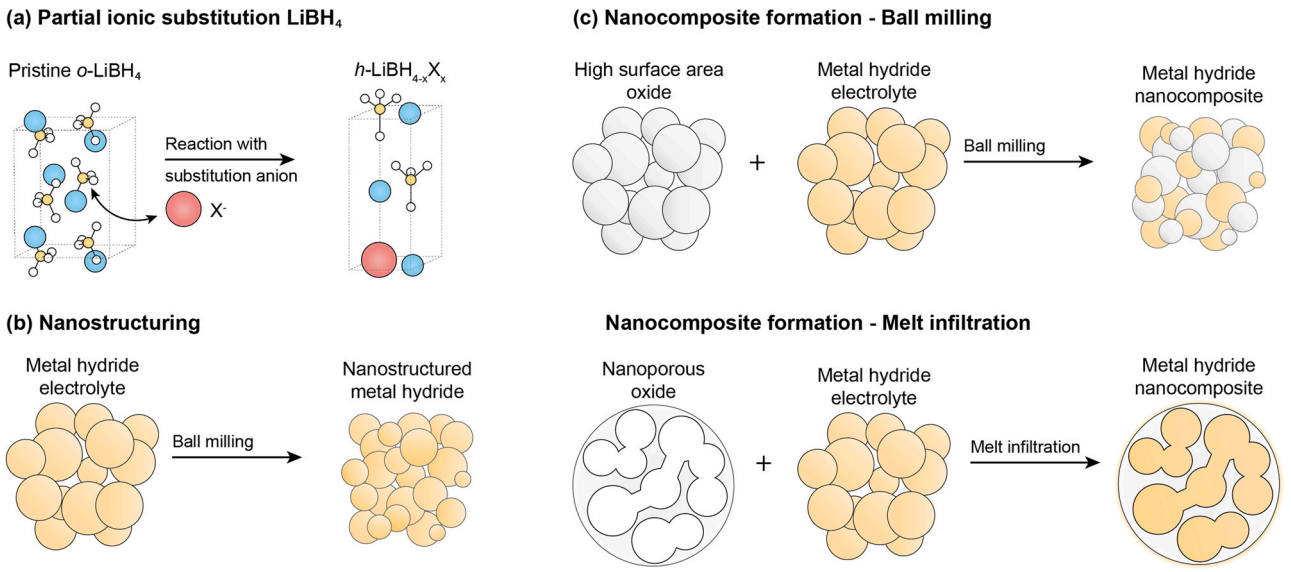

Fig. 3. Schematics of the different strategies that can be used to enhance ionic conductivity in metal hydrides: (a) partial ionic substitution, (b) nanostructuring and (c) nanocomposite formation.

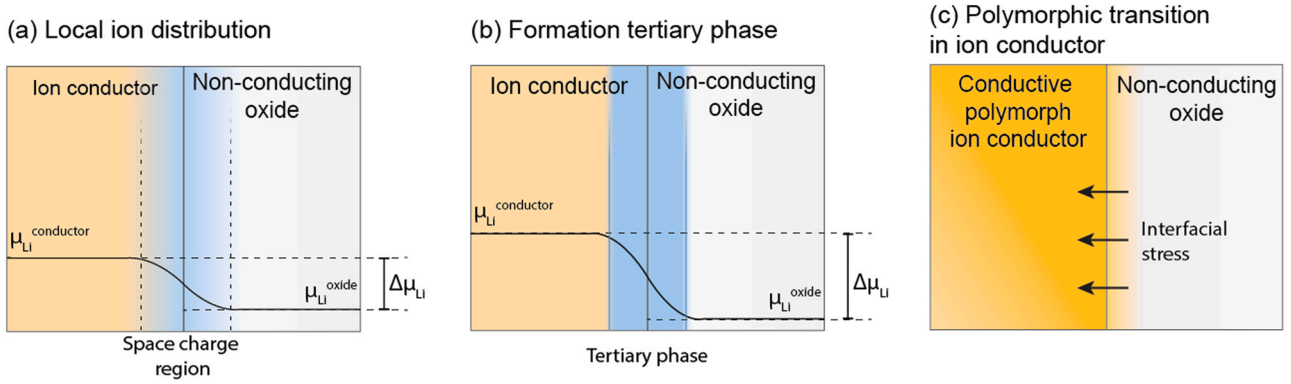

Fig. 4. Schematic illustration of the different interfacial interactions occurring in nanocomposite ion conductors. Fast ionic transport in composite solid electrolytes can be induced by (a) the formation of a space charge layer, (b) the formation of a tertiary phase at the conductor-insulator interface or (c) stabilization of a conductive polymorph of the ion conductor. Copyright 2021 American Chemical Society.
Illustration adapted with permission from ref [38].

the formation of a highly conductive percolating path in a composite solid electrolyte. These diffusion processes can occur within the ionic conductor, within the non-conducting oxide scaffold and across and/or along the conductor-oxide interface. The addition of dispersed scaffold particles in the ion conductor introduces interfacial stress between the conducting and non-conducting components, which can influence the local ion distribution. It can also lead to the formation of a third compound at the ion conductor-oxide interface or even induce a polymorphic transition in the conducting component. These modifications may lead to highly conductive compounds and hence additional conductive paths for ion transport. To illustrate this, a schematic representation of the different ion transport enhancement mechanisms in composite solid electrolytes is provided in Fig. 4.

Typically, the interaction between the insulating scaffold and the ion-conducting compound can result in local ion redistribution, or a space-charge region, while the bulk components remain unaffected (Fig. 4a) [38]. The modified defect thermodynamics close to the ion conductor-scaffold interface can be described by the space-charge model as proposed by Maier. In short, the discontinuity at the interface leads to deviations from local electroneutrality and consequently the formation of a space-charge zone where the concentration of the charge carrying defects is modified and the conductivity is influenced accordingly [96,97].

The space charge model is often used to explain an increase of ionic conductivity in composite solid electrolytes. However, if the local redistribution of ions is not sufficient to compensate for structural mismatches (or large differences in chemical potential) between the conducting and non-conducting components, chemical reactions may occur at the interface. In this case, a third compound is formed at the interface with a structure that is intrinsically different from the ion conductor and the insulating scaffold. This new interphase compound is generally highly defected, and possibly more conductive compared to the starting compounds (Fig. 4b) [38]. Unfortunately, few studies have been reported on this topic, likely because the interphase compounds are difficult to characterize due to their amorphous nature and nanometric thickness.

Besides the formation of a tertiary phase at the conductor-insulator interface, strong interfacial stresses may also lead to (polymorphic) transitions in the ion conducting host (Fig. 4c) [38]. Some ion conductors can exist in different polymorphs with distinctly different transport properties. For these compounds, inclusion of dispersed oxides may alter the stability and consequently the crystallographic structure. For example, a conductive polymorph that is normally stable only at elevated temperatures, can become stable at

ambient temperature due to a depression of the polymorphic transition temperature. This phenomenon has been observed both in polymer-based nanocomposites (e.g. PEO/Al_2O_3 nanocomposites) and in inorganic-based nanocomposites (e.g. AgI/Ag_3BO_3, nano-confined $LiBH_4$). Note that in the latter case a large interfacial stress is often induced by nanoconfinement of the ion conductor in a mesoporous scaffold. In this case, the phase transition temperature of the confined materials (T_m) depends on the size of the confining pore (r_{eff}) following the Gibbs-Thomson equation,

$$\Delta T = T_0 - T_m (r_{eff}) = (2 T_0 (\gamma_{ws} - \gamma_{wl})\nu_l) / (\Delta H_m r_{eff}), \quad (1)$$

where T_0 is the bulk melting temperature, ΔH_m is the melting enthalpy, ν_l is the molar volume of the liquid and γ_{ws} and γ_{wl} are the pore wall-solid and pore wall-liquid interface energies [98]. In general, for each conduction enhancement mechanisms in composite solid electrolytes discussed here, the interaction of the solid electrolyte with the insulating scaffold plays a key role. This has also been observed for complex metal hydride nanocomposites [92,99,100].

To summarize, nanostructuring and nanocomposite formation are interesting methods that offer the possibility to improve the electrochemical properties of metal hydrides and solid-state ion conductors in general. The application of these methods to complex metal hydrides has not been specifically reviewed. Therefore, the design and fabrication of nanostructured and nanocomposite metal hydride-based solid electrolytes will be extensively discussed in the following sections.

3.1. Nanostructured metal hydrides

In this section the effect of nanostructuring on ion mobility in borohydrides, i.e., $LiBH_4$, and *closo*-(car)borates, including $Li_2B_{12}H_{12}$, $Na_2B_{12}H_{12}$, and $NaCB_{11}H_{12}$, will be discussed in detail.

3.1.1. Nanostructured borohydride

Sveinbjörnsson et al. were among the first to report on the effect of nanostructuring on the ionic conductivity in complex metal hydrides, in this case $LiBH_4$ [89]. In their study, pure $LiBH_4$ was ball milled for 2 h, after which $LiBH_4$ was still in the poorly conducting orthorhombic polymorph. By combining information obtained from XRD and impedance spectroscopy, they observed that defect-rich microstructures had formed during the milling process. As a result, the room temperature conductivity of ball milled $LiBH_4$ is almost 3 orders of magnitude larger than non-milled $LiBH_4$, which is shown in the conductivity plot in Fig. 5a. Unfortunately, the defects that formed during ball milling were not thermally stable, hence after heating to 140 °C, the room temperature conductivity decreased to 10^{-7} S cm^{-1}. Interestingly, after the thermal treatment, not all the defects disappeared, and the ionic conductivity of the ball-milled sample was still higher than that of the as-received $LiBH_4$.

These results were corroborated by studies performed by Matsuo et al., Gulino et al. and Epp et al. [29,36,92] It was confirmed that the conductivity of $LiBH_4$ is enhanced significantly upon ball milling, but it is not preserved after heating to 130 – 160 °C. In their study, Gulino et al. reported a similar observation of increased ionic conductivity and showed that the activation energy for the ball-milled $LiBH_4$ (0.70 eV) is smaller than that of pristine $LiBH_4$ (0.91 eV), which increases to 0.75 eV upon heat treatment [92]. Epp et al. studied the effect of nanostructuring on the lithium-ion dynamics in nanostructured $LiBH_4$ with a crystallite domain size of 20 nm in detail using Li NMR spectroscopy. Similar to previously discussed impedance results, their NMR analysis indicates the presence of fast Li ions in nanostructured $LiBH_4$. The authors suggested that this may be attributed to the preservation of the highly conducting hexagonal polymorph in the interfacial regions of the nanostructured material [36], or other structural modifications that lead to an increased defect concentration [92]. From these studies, it can be concluded that nanostructuring by ball milling can induce a large increase in room temperature conductivity in $LiBH_4$, which results from the formation of high defect concentration due to the mechanical milling, and possible stabilization of the hexagonal polymorph as evidenced by the decrease in activation energy [92]. However, as the conductivity depends on non-stable defects, the thermal (and likely the long term) stability remains an issue. For application of $LiBH_4$ in an ASS battery, it will therefore be important to stabilize the highly conductive phase formed in nanostructured $LiBH_4$.

3.1.2. Nanostructured closo-borates and closo-carborates

Metal hydride compounds based on *closo*-borate and *closo*-carborate anions, e.g., $B_{12}H_{12}^{2-}$ and $CB_9H_{10}^-$, were introduced in Section 2.3. Similar to $LiBH_4$, these compounds display high ionic mobilities above a certain polymorphic transition temperature. Recently, several studies have shown that their high ionic conductivity can be stabilized at room temperature using nanostructuring. The effect of nanostructuring on the Li-ion conductivity of $Li_2B_{12}H_{12}$ was studied by Teprovich et al., Tang et al., and Kim et al. [37,91,101] Nanostructured $Li_2B_{12}H_{12}$ was obtained after ball milling for varying times ranging from 10 min to 20 h, in some cases followed by a thermal treatment. To illustrate the effect of ball milling on morphology, SEM images of pristine and ball milled $Li_2B_{12}H_{12}$ are provided in Fig. 5b (1 and 2). Despite the differences in synthesis procedures, all three studies reported that the conductivity of ball milled $Li_2B_{12}H_{12}$ is larger compared to the pristine material. For instance, Kim et al. determined for pristine and nanostructured $Li_2B_{12}H_{12}$ that the ionic conductivity improves by three orders of magnitude, as can be seen in Fig. 5a [91].

Detailed compositional characterization with ICP and a hydrogen analyzer revealed that simple ball milling generates lithium and hydrogen deficiencies. The authors proposed that these deficiencies are generated via the extraction of small amounts of lithium and hydrogen as various types of compounds such as Li, H_2 and LiH. On the basis of structural characterizations, it is speculated that the atom deficiencies lead to an increased carrier concentration, which in turn results in an improved lithium-ion conductivity [91]. Another explanation is the room temperature stabilization of the high conductivity disordered polymorph normally obtained after the reversible polymorphic phase transition at 350 °C [37]. Unfortunately, the changes induced during ball milling (either via atom deficiencies or polymorphic phase stabilization) are not stable at higher temperatures. Tang et al. reported that the enhanced ion conductivity in ball milled $Li_2B_{12}H_{12}$ is not sustained after heating to 140 °C, similar to the behaviour observed for nanostructured $LiBH_4$ [37]. The structure/morphology of the nanostructured material is not sufficiently robust at high temperatures. Hence, for nanostructured $Li_2B_{12}H_{12}$ (and other nanostructured metal hydrides affected by heating) it is essential to avoid high temperatures. In this way, sintering processes that degrade conduction properties within the life cycle of an all-solid-state battery, might be avoided.

Interestingly, nanostructured $Na_2B_{12}H_{12}$ displays intriguing behaviour upon temperature cycling, different from nanostructured $LiBH_4$ and $Li_2B_{12}H_{12}$. Tang et al. prepared nanostructured $Na_2B_{12}H_{12}$ by ball milling for 72 h [37]. As can be seen in Fig. 5b (3 and 4), ball milling results in crystal grain pulverization, similar to what is observed in $Li_2B_{12}H_{12}$. Phase analysis of the nanostructured material by Rietveld refinement reveals the presence of two phases, the expected low temperature ordered polymorph and a second, higher symmetry disordered phase that is similar to the polymorph normally present above the order-disorder phase transition temperature. In Fig. 5a the ionic conductivities of $Na_2B_{12}H_{12}$ pre- and post-ball milling are compared. Clearly, ball milling leads to a profound conductivity increase of four orders of magnitude. Remarkably, this conductivity enhancement persists during several heating cycles,

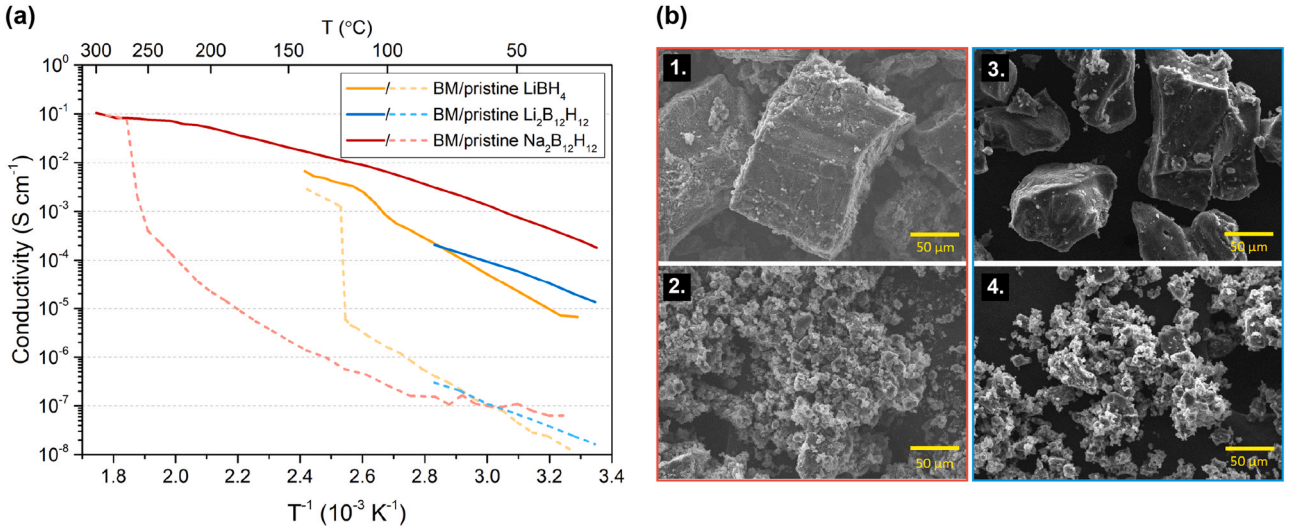

Fig. 5. (a) Arrhenius plot of the conductivity of pristine and ball milled metal hydrides [37,65,89,91]. (b) SEM images of (1) pristine $Na_2B_{12}H_{12}$, (2) nanostructured $Na_2B_{12}H_{12}$ (ball milled for 72 h), (3) pristine $Li_2B_{12}H_{12}$ and (4) nanostructured $Li_2B_{12}H_{12}$ (ball milled for 20 h). Copyright 2016 Elsevier.
Data is reprinted with permission from ref [37].

even after heating to 350 °C. Thus, compared to $Li_2B_{12}H_{12}$ and $LiBH_4$, nanostructured $Na_2B_{12}H_{12}$ seems to form a more stable conductive material that is less likely to deteriorate during battery operation.

The effect of mechanical milling on the phase behavior of several other lithium and sodium *closo*-(car)borate compounds, including $Li_2B_{10}H_{10}$, $Na_2B_{10}H_{10}$, $LiCB_{11}H_{12}$ and $NaCB_{11}H_{12}$, was probed in the same study [37]. In general, for all investigated compounds it was found that crystallite size reduction and disordering effects led to the room temperature stabilization of the superionic conducting polymorphs normally present at higher temperatures. This illustrates that nanostructuring is a viable strategy to induce high cation mobilities in these metal hydride-based ion conductors. However, for most nanostructured metal hydrides (except for $Na_2B_{12}H_{12}$) a large decrease in conductivity is observed after heating to elevated temperatures. It would therefore be interesting to find a way to preserve the nanostructured phases, for example through the formation of a nanocomposite with a (non-conducting) oxide nanoscaffold, such as SiO_2 or Al_2O_3. The influence of nanocomposite formation (and interface engineering) on the conductivity in metal hydrides will be extensively discussed in the next section.

3.2. Metal hydride/metal oxide nanocomposites

In the previous section, the application of nanocomposite formation was proposed as a method to improve the stability of nanostructured metal hydrides. In addition to the nanostructuring effects, interface interactions between the oxide scaffold and nanostructured metal hydride could affect the ion diffusivity in the nanocomposites, as explained in the beginning of this chapter. In this section, the effect of nanocomposite formation on ionic mobility in pure metal hydrides, i.e. $LiBH_4$, $NaBH_4$ and $Li_2B_{12}H_{12}$, as well as partially ion substituted metal hydrides, i.e. $LiBH_4$-LiI and $LiBH_4$-$LiNH_2$, will be reviewed.

3.2.1. Borohydride/oxide nanocomposites

In 2012, Verkuijlen and co-workers observed highly mobile Li^+-ions upon melt infiltration of $LiBH_4$ in a mesoporous SiO_2 scaffold (MCM-41) [102]. Their static ^7Li and ^{11}B NMR measurements demonstrated that the mobility of both Li^+ and BH_4^- is strongly increased after nanoconfinement. In a subsequent study by Blanchard et al., it was shown for the first time that confining $LiBH_4$ in the pores of ordered mesoporous silica scaffolds leads to high Li^+ conductivity of 0.1 □ 10^{-3} S cm^{-1} at room temperature, as displayed in Fig. 6a [95]. The Nyquist plots obtained with Electrochemical Impedance spectroscopy measurements at 30 °C, 50 °C and 80 °C consist of single, slightly depressed semi-circles, which suggests that the ionic conduction in the nanoconfined $LiBH_4$, or $LiBH_4/SiO_2$ nanocomposite, is governed by only one diffusion process. Notably, upon nanocomposite formation the activation energy for lithium diffusion was reduced accordingly, from 0.55 eV (*h*-$LiBH_4$) to 0.43 eV. In contrast to nanostructured $LiBH_4$, the conductivity of the $LiBH_4/SiO_2$ nanocomposite is very stable in time and against temperature changes. Furthermore, the authors proposed that the high ionic mobility originates from a fraction of the confined borohydride that is located close to the interface with the SiO_2 pore walls, a conductive interfacial layer of about 1.0 nm thickness (Fig. 6b) [95]. Subsequent studies confirmed that interface interactions between $LiBH_4$ and the mesoporous SiO_2 scaffold are essential to the high conductivity in $LiBH_4/SiO_2$ nanocomposites obtained via melt infiltration [103,104]. However, while the formation of the interfacial layer was verified, it was found that the thickness of the interfacial layer is 1.9 – 2.0 nm [92,105].

The conductivity of $LiBH_4/SiO_2$ nanocomposites obtained via ball milling has been investigated as well. Choi et al. prepared composites of $LiBH_4$ and two different types of high surface area SiO_2 (MCM-41 and fumed SiO_2) with high-energy ball milling. The ion conductivity of the composites ranged from 10^{-5} S cm^{-1} (MCM-41) to 10^{-4} S cm^{-1} (fumed SiO_2) at room temperature. Interestingly, by employing a continuum percolation model, the conductivity of the $LiBH_4/SiO_2$ interface layer was estimated to be 10^5 times higher than that of pure macrocrystalline $LiBH_4$ [106]. The conductive interface layer is likely the result of a reaction between the surface silanol groups and the confined $LiBH_4$, as suggested by Lefevr et al. for ball milled $LiBH_4/SiO_2$ aerogel [107]. Both studies highlight the importance of the interface and indicate that significant enhancement in ionic conductivity can be achieved via nanocomposite formation, both with melt infiltration and ball milling.

The Li-ion mobility in $LiBH_4$/oxide nanocomposites can be improved by maximizing the contact area between $LiBH_4$ and the oxide, or by optimizing the interaction between the components, for example by changing the density or nature of the active surface groups. Since the nature and density of surface groups differs greatly between different oxide scaffolds, using a different oxide could affect the conductivity of $LiBH_4$ nanocomposite electrolytes. In fact, Choi

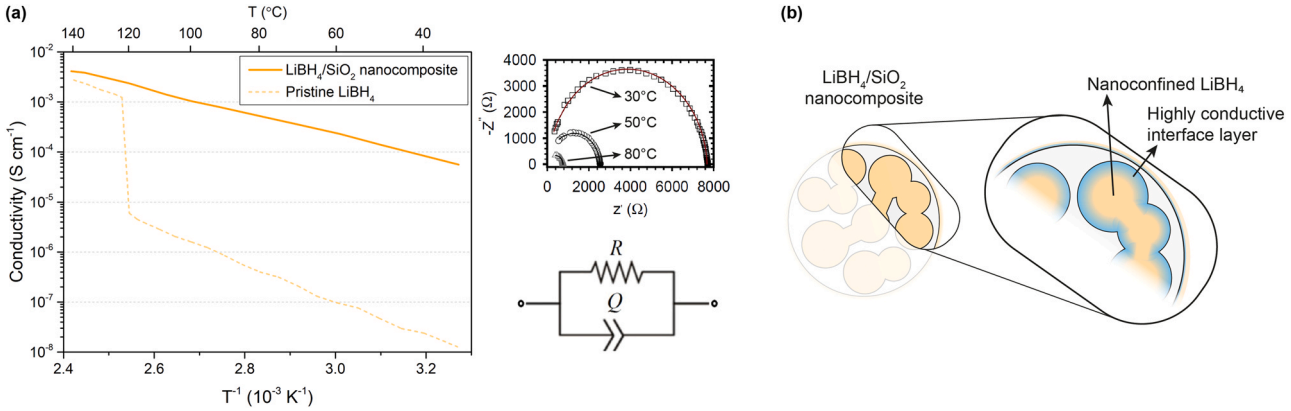

Fig. 6. (a) Arrhenius plot of the conductivity of pristine and nanoconfined $LiBH_4$, including Nyquist plots of the $LiBH_4/SiO_2$ nanocomposite obtained at 30 °C, 50 °C and 80 °C. Copyright 2015 Wiley.
Data is reprinted with permission from ref [95]. (b) Schematic visualization of the metal hydride-metal oxide interface layer.

et al. demonstrated that Al_2O_3 is more effective in making a highly conducting interface layer in ball-milled $LiBH_4$/oxide nanocomposites than the previously investigated SiO_2 [99]. The ionic conductivity of their $LiBH_4/Al_2O_3$ nanocomposite reaches a value of $2 \cdot 10^{-4}$ S cm^{-1}, which is twice as high as that of the $LiBH_4/SiO_2$ nanocomposite. For the $LiBH_4/Al_2O_3$ nanocomposite, the formation of an interfacial layer was confirmed by near-edge X-ray absorption, which revealed the presence of B-O bonds in the nanocomposite. Likewise, in a recent study by Dou et al. $LiBH_4$ nanocomposites were prepared based on layered double hydroxides (LDHs), high surface area materials with a high density of active surface hydroxyls [108]. By using LDHs as insulating scaffold, the interface interaction with $LiBH_4$ could be maximized, which resulted in a remarkable increase in ionic conductivity. For example, $LiBH_4$/MgAl-LDH nanocomposites exhibited a five order of magnitude increase in room temperature conductivity, reaching values up to $0.31 \cdot 10^{-3}$ S cm^{-1}. For both studies the enhancement in conductivity could be explained by a higher density of surface hydroxyl groups in the scaffold compared to SiO_2 resulting in a more conductive interface layer with more B-O bonds and more mobile Li ions. Note that the exact mechanism for B-O bond formation is still under debate. It has been speculated that a SiO-BH_3Li species forms upon partial reaction of $LiBH_4$ with the surface hydroxyl groups.

The effect of the nature of the oxide scaffold on $LiBH_4$ nanocomposite conductivity was explored systematically [92]. In this study, $LiBH_4$/oxide nanocomposites were prepared through ball milling with various nanosized oxides, including SiO_2, Al_2O_3, CaO, MgO and ZrO_2. In all cases, 25 v/v% of oxide was present in the nanocomposites. The ionic conductivity of the nanocomposites was greatly enhanced for all oxides (Fig. 7a). Notably, preparation with ZrO_2 and MgO resulted in the most conductive nanocomposite electrolytes, with conductivities of 0.26 and 0.18 □ 10^{-3} S cm^{-1} at 40 °C, respectively. These values are more than four orders of magnitude higher than that of macrocrystalline $LiBH_4$, and also clearly higher than those observed for the SiO_2- and Al_2O_3-based nanocomposites prepared in the same manner. The activation energies for ionic transport also depend on the oxide that is used. The lowest activation energies, 0.44 and 0.46 eV, were observed for ZrO_2 and MgO-containing nanocomposites, while the nanocomposites based on SiO_2 and Al_2O_3 show activation energies of 0.52 and 0.55 eV. Based on their results the authors deduced a set of design rules to optimize the influence of the oxide on the overall conductivity [92]. This study demonstrates that interface engineering is an effective strategy to improve nanocomposite conductivity, especially by choosing the optimal oxide scaffold and optimizing overall composition. Likewise, a recent study has illustrated that besides oxidic scaffolds, high surface area, two-dimensional layered MoS_2 could

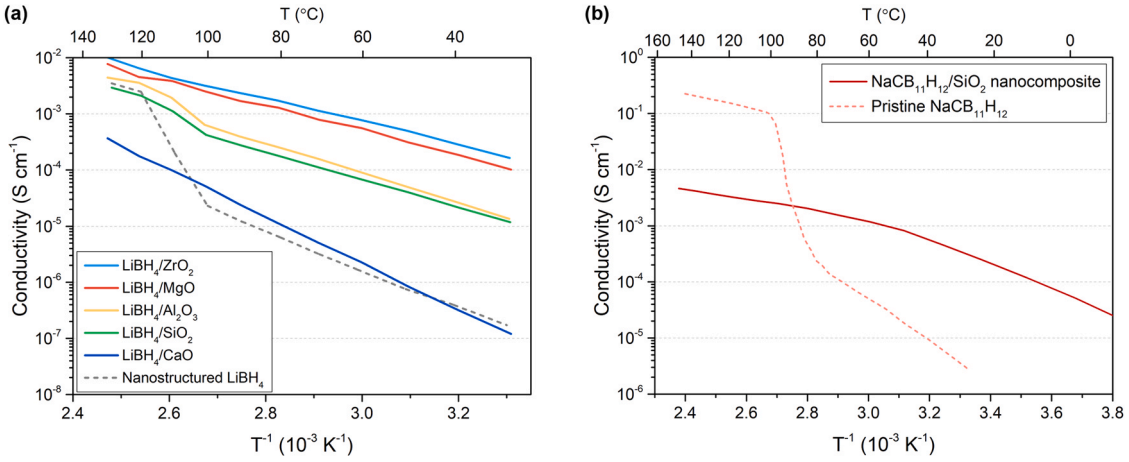

Fig. 7. (a) Li-ion conductivity of ball milled mixtures of $LiBH_4$ with 25 v/v% of different oxides. Copyright 2020 American Chemical Society. (b) Na-ion conductivity of pristine $NaCB_{11}H_{12}$ and $NaCB_{11}H_{12}$ nanoconfined in a SiO_2 scaffold using 130% pore filling. Copyright 2021 American Chemical Society.
(a) Data is adapted with permission from ref [92]. (b) Data is adapted with permission from ref [111].

also be considered as promising nanocomposite scaffold [109]. The novel $LiBH_4/MoS_2$ nanocomposite reported in this work exhibited a room temperature conductivity of 10^{-4} S cm^{-1}, further broadening the possibilities of interface engineered $LiBH_4$ to include sulfide-based scaffolds as well. Note that additional studies are required to determine which scaffold property, e.g., surface chemistry, acidity, or physical structure (morphology, particle size and porosity), is essential to the formation of a conductive interface.

While several studies have shown the profound benefits of nanocomposite formation on the ionic conductivity of $LiBH_4$, studies on other metal hydride ion conductors, such as alanates and amines, are scarce. It has only recently been determined that nanocomposite formation can also be applied to tune the properties of sodium-based metal hydrides, though for these compounds the strategy seems less effective [59]. In fact, upon melt infiltration of $NaBH_4$ in mesoporous SiO_2 (MCM-41) a limited improvement in ionic conductivity of just one order of magnitude is observed between 20 °C and 70 °C. The small enhancement in conductivity is attributed to the formation of $Na_2B_{12}H_{12}$ in the pores of the scaffold upon nanoconfinement. Moreover, both IR and NMR analysis demonstrate the formation of B-O bonds, similar to $LiBH_4/Al_2O_3$ [99]. This indicates that like interface engineered $LiBH_4$ an interface layer is formed at the metal hydride-metal oxide interface, though it is not highly conductive in the case of $NaBH_4/SiO_2$ [59]. Therefore, nanoconfined $NaBH_4$ might benefit greatly from the application of other scaffolds that could introduce stronger interface interactions. Indeed, by using MgAl-layered double hydroxides(LDHs) in $NaBH_4$-based nanocomposites, Dou et al. were able to achieve a conductivity increase of three orders of magnitude [108]. The hydroxyl rich surface of the LDHs enhances the interface interaction between $NaBH_4$ and the scaffold, thereby promoting defect formation and Na^+ ion diffusion. It is thus clear that nanocomposite formation is very effective in enhancing conductivity in both $LiBH_4$ and $NaBH_4$, however, especially for the latter it is important to maximize interface interaction between the metal hydride and the non-conducting scaffolds.

3.2.2. *Closo-borate- and closo-carborate/oxide nanocomposites*

In Section 3.1.2, it has been shown that nanostructuring is a viable technique to enhance cation mobilities in *closo*-borates and *closo*-carborates. On the other hand, the conductivity of nanostructured *closo*-(car)borates is not (thermally) stable and decreases significantly after heating to high temperatures. Nanocomposite formation might offer a way to stabilize the high conductivity in nanostructured *closo*-(car)borate-based solid electrolytes.

Recently, Yan et al. prepared nanocomposites with $Li_2B_{12}H_{12}$ using mesoporous SiO_2 as scaffold [110]. Since $Li_2B_{12}H_{12}$ has a high melting point (T_m > 500 °C), the composite cannot be simply formed via melt infiltration. Hence, a two-step synthesis method was applied in which firstly nanoconfined $LiBH_4$ was prepared, after which the confined $LiBH_4$ was treated with a H_2/B_2H_6 atmosphere at 150 °C to form nanoconfined $Li_2B_{12}H_{12}$. It was confirmed with ^{11}B MAS NMR that all $LiBH_4$ is successfully converted to 94 mol% $Li_2B_{12}H_{12}$ and 6 mol% $Li_2B_{10}H_{10}$. Unfortunately, the as-synthesized nanocomposite exhibits a low ionic conductivity of $1.0{\cdot}10^{-7}$ S cm^{-1} at 25 °C, similar to the value obtained for bulk $Li_2B_{12}H_{12}$ [110]. It should be considered that the preparation method might affect the formation of a conductive interface layer between the metal hydride and the oxide. As a result, the $Li_2B_{12}H_{12}$/oxide nanocomposite might display a limited Li-ion mobility, in contrast to interface engineered $LiBH_4$. This study does not firmly resolve whether nanocomposite formation can help stabilize the high-temperature superionic polymorph of (car)borate metal hydrides or improve their room temperature conductivity. Therefore, it would be interesting to compare the conductivities of $Li_2B_{12}H_{12}$ nanocomposite prepared via this method, to a $Li_2B_{12}H_{12}/SiO_2$ nanocomposite synthesized through other methods, such as high-energy ball milling.

In a recent study by Andersson et al. a novel approach was proposed to prepare *closo*-(car)borate nanocomposites [111]. In their work, nanodispersion of $NaCB_{11}H_{12}$ in porous SiO_2 was achieved via salt-solution infiltration followed by vacuum desolvation, an approach similar to melt infiltration. Structural characterizations with DSC and XRD indicate that the metal hydride was confined in the scaffold pores. This nanoconfined $NaCB_{11}H_{12}$ phase resembled the high-temperature superionic polymorph of bulk $NaCB_{11}H_{12}$, with dynamically disordered $CB_{11}H_{12}^-$ anions exhibiting fast reorientational mobility. The high anion mobilities promote fast cation diffusion, which yields Na-ion conductivities of $0.3{\cdot}10^{-3}$ S cm^{-1} at room temperature (Fig. 7b). Notably, it is expected that the conductivity of the $NaCB_{11}H_{12}/SiO_2$ nanocomposite can be further improved by optimization of the preparation method, for example by applying ball milling or improving the solution impregnation method, as well as tuning of the nanocomposite composition, e.g., by scaffold chemistry and volume fraction. Nevertheless, this work demonstrates that the formation of a nanocomposite is a viable strategy to stabilize highly conductive phases not only in borohydride-based compounds, but also in *closo*-(car)borate-based solid electrolytes.

3.2.3. *$LiBH_4$-LiI/oxide nanocomposites*

In the previous sections, the application of nanocomposite formation on macrocrystalline metal hydrides was discussed. However, this method might also lead to an enhanced conductivity in ion substituted metal hydrides, such as $Li(BH_4)_{1-x}I_x$ or $Li_2(BH_4)(NH_2)$. In this way, synergetic effects of both enhancement strategies (ion substitution, nanostructuring and interfacial effects) could lead to even greater improvement of the ionic mobility. Recently, this type of solid-state ion conductors has been explored in detail.

In 2019, Lu et al. were the first to report on the synthesis of a highly conductive $Li_4(BH_4)_3I/SiO_2$ nanocomposite by confining the LiI-substituted $LiBH_4$ into mesoporous silica (SBA-15). The authors prepared the most conductive $LiBH_4$-LiI solid solution, $Li_4(BH_4)_3I$, as reported by Miyazaki et al. [80] The phase composition of the $LiBH_4$-LiI solid solution and the nanocomposite were characterized with XRD. At room temperature, $Li_4(BH_4)_3I$ was in the hexagonal P63mc polymorph. After melt infiltration of the $Li_4(BH_4)_3I$ solid solution in the mesoporous SiO_2 scaffold, the corresponding diffraction peaks became less intense [112]. This indicates that the hexagonal polymorph of $Li_4(BH_4)_3I$ was stabilized in the pores of the amorphous SiO_2. The temperature-dependent conductivities of $LiBH_4$, $Li_4(BH_4)_3I$ and nanoconfined $Li_4(BH_4)_3I$ are depicted in Fig. 8a. Here, it can be seen clearly that $Li_4(BH_4)_3I$/oxide nanocomposite exhibits significantly enhanced conductivity of $2.5{\cdot}10^{-4}$ S cm^{-1} at 35 °C, compared to the pristine $Li_4(BH_4)_3I$ solid solution and the nanoconfined $LiBH_4$. Based on ^{7}Li solid-state NMR measurements, it was proposed that an interface layer with a thickness of 1.2 nm between $Li_4(BH_4)_3I$ and SiO_2 is responsible for the fast Li-ion conduction [112]. Note that this value is similar to the interface layer thickness of 1.9 nm calculated for $LiBH_4$/oxide nanocomposites [105]. These results reveal that the conductivity of $LiBH_4$ can be further improved by synergetic effects of partial ionic substitution and nanoconfinement.

Since the conductivity enhancement in $Li_4(BH_4)_3I/SiO_2$ nanocomposites originates from the formation of a conductive interface layer, the type of oxide could affect the nanocomposite conductivity. Zettl et al. studied the conductivity of $LiBH_4$-LiI confined in mesoporous SiO_2 and Al_2O_3, where $Li_4(BH_4)_3I$ was formed in-situ during melt infiltration in the scaffold [113]. Their study confirmed that the interaction of $LiBH_4$ with the oxide interface is crucial for the enhancement of the ionic conductivity. A preparation technique that hindered the interaction of $LiBH_4$ with the oxide interface, whilst still forming $LiBH_4$-LiI in the oxide pores, was employed. In this case, $LiBH_4$-LiI/oxide nanocomposites exhibited much lower conductivities than those in which interface interaction was possible. On the other hand, when comparing $LiBH_4$-LiI/SiO_2 and $LiBH_4$-LiI/Al_2O_3

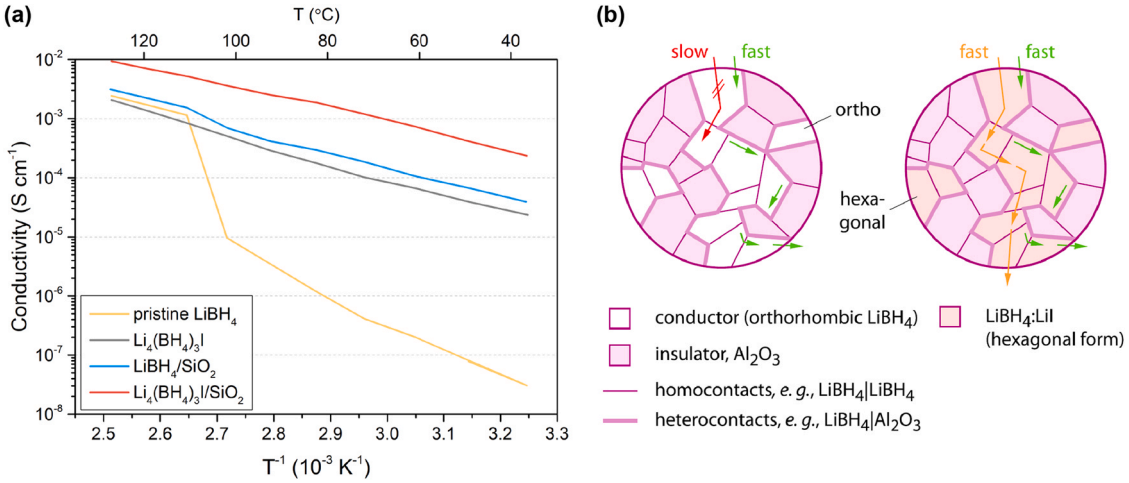

Fig. 8. (a) Temperature-dependent Li-ion conductivities of $LiBH_4$, $Li_4(BH_4)_3I$ and $Li_4(BH_4)_3I/SiO_2$. Copyright 2019 Wiley. (b) Schematic representation of a system composed of a nanocrystalline ionic conductor ($LiBH_4$ or $LiBH_4$-LiI) and a nanocrystalline insulator (Al_2O_3). Copyright 2021 American Chemical Society.
(a) Data is adapted with permission from ref [112]. (b) Schematic reprinted with permission from ref [116].

nanocomposites, it was found that they displayed very similar conductivities ($1.3{\cdot}10^{-4}$ S cm^{-1} at 25 °C) and activation energies for Li-ion transport (0.44 eV in both cases). It is important to note here that the SiO_2 (SBA-15) and Al_2O_3 scaffold are different in terms of morphology, porosity and surface chemistry, which makes it impossible to identify the exact influence of the different scaffold properties on ionic conductivity. Hence, detailed NMR studies were required to determine the underlying principles of Li^+-conduction in ion substituted $LiBH_4$/oxide nanocomposites, and the effect of surface interactions on the conduction mechanism.

To this end, in a subsequent study broadband conductivity spectroscopy and ^1H, ^6Li, ^7Li, ^{11}B, and ^{27}Al NMR was used to study structural and dynamic features of nanoconfined $LiBH_4$-LiI/Al_2O_3 [114]. In particular, interfacial effects were clearly observed by ^{27}Al magic angle spinning NMR. Notably, it is observed that penta-coordinated Al sites of the Al_2O_3 scaffold becomes saturated through the formation of either $Li^+[AlO_5I]^-$ or $Li^+[AlO_5BH_4]^-$ species, possibly via reaction with surface hydroxyl groups [114]. A $Li^+[AlO_5X]^-$ complex could leave behind Li^+ vacancies in the surface regions, thereby generating enhanced diffusion through hopping processes. Similar to LiF/Al_2O_3 [115], these percolating surface pathways would give rise to enhanced long-range Li ion transport [114]. Such a surface-controlled diffusion mechanism might be a universal feature of conductor/insulator composites, in particular with Al_2O_3.

In a follow-up study, the authors employed variable-temperature ^7Li NMR spectroscopy to quantify the effect of the conductor-insulator interfacial regions in nanoconfined $LiBH_4/Al_2O_3$ and $LiBH_4$-LiI/Al_2O_3 [116]. The study provided an additional proof that penta-coordinated Al centers near the Al_2O_3 surfaces are involved in creating a defect rich $LiBH_4$(-LiI)/Al_2O_3 interface. It was shown that the interfacial regions in the $LiBH_4$(-LiI)/Al_2O_3 nanocomposites display extremely rapid ^7Li NMR spin fluctuations, which provides direct evidence for fast Li^+ jump processes in both nanoconfined $LiBH_4/Al_2O_3$ and $LiBH_4$-LiI/Al_2O_3. The fact that almost no difference is seen between the ^7Li NMR spin fluctuations of the nanocomposites reveals that the lithium dynamics in the conductive interface regions are independent of the $LiBH_4$ polymorph, either being orthorhombic ($LiBH_4$) or hexagonal ($LiBH_4$-LiI). Thus, the interfacial regions play a dominant role in explaining the enhanced ion dynamics in the nanoconfined samples, regardless of whether LiI is present or not. On the other hand, these results do not explain why long-range ionic transport in $LiBH_4$-LiI/Al_2O_3 is faster than in $LiBH_4/Al_2O_3$. Most likely, the difference originates from the orthorhombic bulk regions in the latter compound. As illustrated schematically in Fig. 8b, the orthorhombic regions in $LiBH_4/Al_2O_3$ limit Li^+ ion transport through long-range ion transport pathways, in contrast to the more conductive hexagonal bulk regions in $LiBH_4$-LiI/Al_2O_3. In summary, in both nanocomposites the interface regions provide fast Li^+ diffusion pathways, however anion substitution ensures fast Li^+ diffusivity in the hexagonal bulk regions that do not benefit from interactions with the oxidic surface regions. In this way, the combination of nanoconfinement and anion substitution enables facile, overall long-range Li-ion transport.

3.2.4. *$LiBH_4$-$LiNH_2$/oxide nanocomposites*

Similar to the previously discussed $LiBH_4$-LiI/oxide nanocomposites, the combination of nanoconfinement and anion substitution with NH_2^- also results in highly conductive nanocomposites. While this system was only concisely discussed in a previous study [113], the $LiBH_4$-$LiNH_2$/oxide nanocomposites were investigated in greater detail by de Kort et al. [100] First of all, it should be noted that partial ionic substitution with NH_2^- leads to the formation of new compounds, including $Li_2(BH_4)(NH_2)$ and $Li_4(BH_4)(NH_2)_3$, unlike $LiBH_4$-LiI in which the high-temperature polymorph of $LiBH_4$ is stabilized [79,117–119]. These new compounds have relatively low melting points [117], e.g. 90 °C for $Li_2(BH_4)(NH_2)$ [119], which results in interesting ion conduction properties. In general, the ionic conductivity of $LiBH_4$-$LiNH_2$ mixtures is higher than that of pure $LiBH_4$. Most striking is the sharp increase in conductivity between 25 °C and 40 °C, which is attributed to the melting of the new compound $Li_2(BH_4)(NH_2)$ [79,100]. At temperatures above 40 °C the conductivity shows negligible temperature dependence, suggesting the formation of a superionic conducting phase [100]. Since $LiBH_4$-$LiNH_2$ displays different conduction behavior compared to $LiBH_4$-LiI, the effect of nanocomposite formation on the conductivity of $LiNH_2$-substituted $LiBH_4$ solid electrolytes might also be different.

Upon melt infiltration in a mesoporous oxide scaffold, either SiO_2 or γ-Al_2O_3, the ionic conductivity of the $LiBH_4$-$LiNH_2$/oxide nanocomposites in enhanced. The highest conductivity of $5{\cdot}10^{-4}$ S cm^{-1} at 30 °C is obtained using mesoporous SiO_2 (SBA-15) as scaffold [100]. In a later study by Yang et al., similar results have been observed for $Li_2(BH_4)(NH_2)$ confined in a mesoporous SiO_2 [120]. In Fig. 9, it can be seen that over the recorded temperature range no phase change-induced conductivity increase can be identified, in contrast to the non-confined $LiBH_4$-$LiNH_2$ mixture [100]. This suggests that the origin of the conductivity enhancement in $LiNH_2$-substituted $LiBH_4$ might be different from other complex hydride nanocomposites, e.g. $LiBH_4$ and $LiBH_4$-LiI. Specifically, the conductivity enhancement

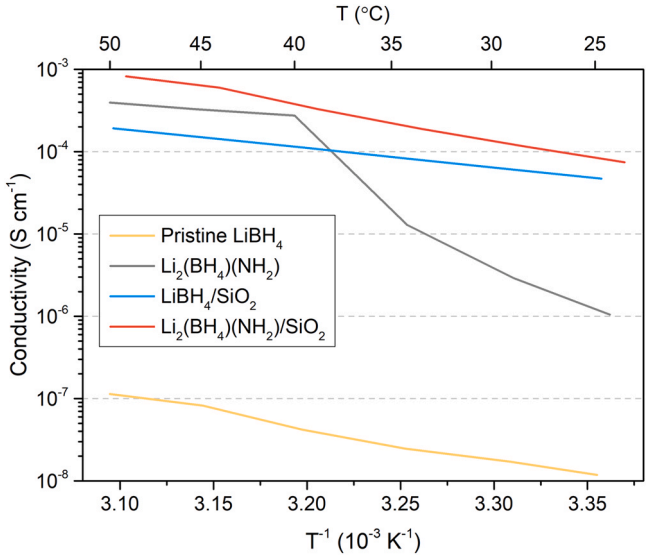

Fig. 9. Ionic conductivity of interface engineered $LiBH_4$-$LiNH_2$/SiO_2 as a function of the reciprocal temperature. For comparison, the conductivity data of $LiBH_4$/SiO_2, non-confined $LiBH_4$-$LiNH_2$ and pristine $LiBH_4$ are included [100].

could be attributed not only to the formation of a highly conductive interface layer, but also to the stabilization of (highly conductive) molten $LiBH_4$-$LiNH_2$ at room temperature due to nanoconfinement effects.

Even though the conductivity enhancement might not be solely related to the formation of a conductive hydride/oxide interface layer, the nanocomposite conductivity could still be affected by the properties of the mesoporous scaffold. Therefore, de Kort et al. systematically investigated the influence of scaffold properties on the conductivity of $LiNH_2$-substituted $LiBH_4$/oxide nanocomposites using metal oxides with different surface chemistry and physical properties (e.g. porosity) [100]. The study reveals that the conductivity of $LiBH_4$-$LiNH_2$/oxide nanocomposites is strongly influenced by both the chemical and physical nature of the scaffold material (Fig. 10). By tuning the surface chemistry (Fig. 10a) and the pore structure (Fig. 10b) of the mesoporous oxide, the nanocomposite conductivity could be varied by three orders of magnitude at room temperature. Surprisingly, the most dominant factor contributing to an improved conductivity in $LiBH_4$-$LiNH_2$/oxide nanocomposites, is the pore volume of the mesoporous oxide (Fig. 10c). This is in contrast to $LiBH_4$/oxide nanocomposite, where the conductivity is governed by the chemical nature of the mesoporous scaffold. Moreover, it is observed that despite the large difference in conductivity, the activation energy for ion transport in the different nanocomposites remains generally the same. The authors suggested that the strong correlation between conductivity and pore volume indicates that the conductivity enhancement in $LiBH_4$-$LiNH_2$/oxide nanocomposites is mostly the result of stabilization of highly conductive molten $LiBH_4$-$LiNH_2$ in the scaffold pores, rather than the formation of a conductive interface layer.

The results were further corroborated by two recent studies by Yan et al. and Zhao et al. [121,122]. Both authors studied a similar system to $LiBH_4$-$LiNH_2$/oxide nanocomposites based on hemi-ammine lithium borohydride ($LiBH_4 \cdot xNH_3$) combined with in-situ formed nanocrystalline Li_2O. Zhao et al. demonstrated that nanocomposite formation with Li_2O enhances the ionic conductivity, thermal stability, and electrochemical properties of $LiBH_4 \cdot xNH_3$ ($x = 0.67 - 0.8$) [122]. In the presence of 78 wt% of Li_2O, $LiBH_4 \cdot xNH_3$ forms a highly conductive amorphous or molten layer on the surface of the Li_2O particles. The authors attribute the stabilization of molten $LiBH_4 \cdot xNH_3$ to the strong interfacial effect of formed nanocrystalline Li_2O, which prevents recrystallisation. It is surprising that this highly conductive composite contains only 22 wt% of active material ($LiBH_4 \cdot xNH_3$), suggesting that Li_2O might be an active additive in this case. Similar results have been reported recently for Mg $(BH_4)_2 \cdot xNH_3$ nanocomposites, in which a conductive molten state could be stabilized with high amounts of nanoparticles (ca. 75 wt%) resulting in a room temperature conductivity around 10^{-5} S cm^{-1} [63]. In the case of $LiBH_4 \cdot xNH_3$, it was suggested that the interface layer between $LiBH_4 \cdot xNH_3$ and Li_2O might further promote the migration of Li-ions. Consequently, the ionic conductivity at 20 °C increases to 5.4 10^{-4} S cm^{-1} and the electrochemical stability window widened from 0.5 to 3.8 V, showing that the interface effects induced a profound change in the structure and electrochemical properties of the composite [122].

From the works described in previous sections, it is clear that the conductivity of monophasic (pristine), as well as ion-substituted metal hydrides can be greatly enhanced via nanocomposite formation and interface engineering. An overview of the discussed metal hydride-based nanocomposites and the corresponding conductivities are provided in Fig. 11. The conductivity of metal hydride-based nanocomposite ion conductors is closely linked to the properties of the scaffold materials. Both the chemical nature and the physical properties (e.g. morphology or porosity) of the non-conducting oxide can influence the overall conductivity and activation energy of ion hopping, though the exact extent depends on the metal hydride. It should be noted that only non-reducible scaffolds can be used in metal hydride-based nanocomposites, as the formation of oxygen vacancies in the oxides, through reduction by the highly reducing hydrides, can induce electrical conductivity [92]. Furthermore, even though electrolyte conductivity has been the focus of this

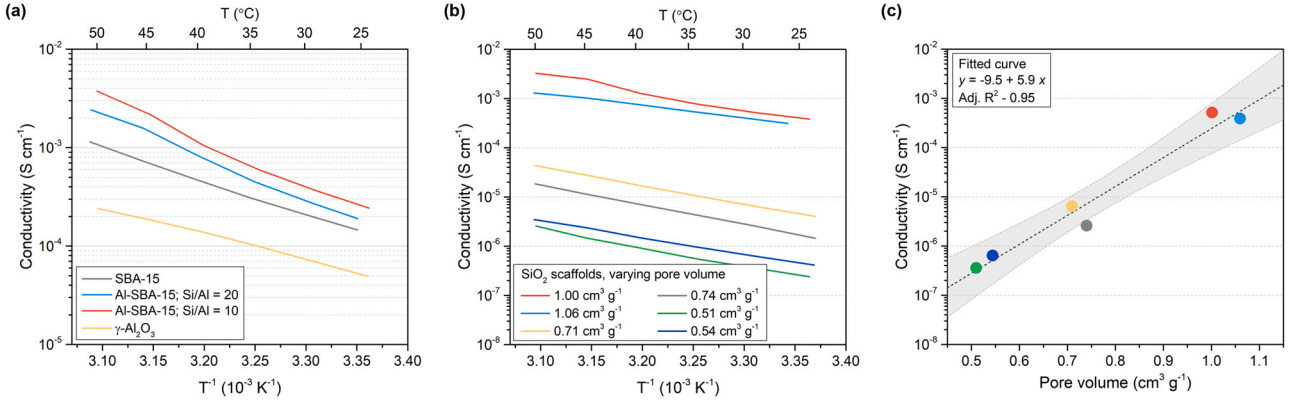

Fig. 10. Temperature-dependent Li-ion conductivity of $LiBH_4$-$LiNH_2$ nanoconfined in scaffolds with (a) different surface chemistry and (b) different porosity. (c) Correlation between nanocomposite conductivity and pore volume of the applied SiO_2 scaffold [100].

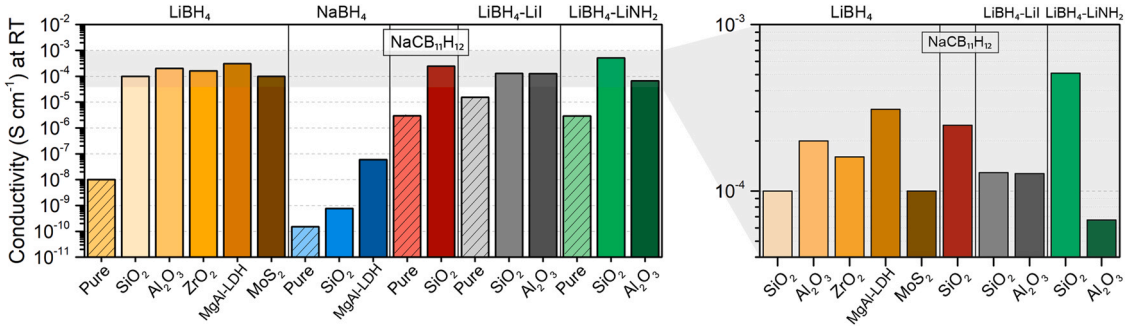

Fig. 11. Overview of the ionic conductivity of the metal hydride-based nanocomposites discussed in this review at room temperature (T = 20 – 30 °C). On the right, an enlargement of the grey area is provided to more clearly distinguish the differences between the most conductive nanocomposites.

review, other electrolyte properties, such as electrochemical stability window and interface stability with electrode materials, are also important properties for practical application in ASS batteries. Hence, in the following section several ASS batteries based on metal hydride nanocomposite electrolytes will be reviewed.

4. All-solid-state batteries based on metal hydride nanocomposite electrolytes

In the following sections, the applicability of metal hydride nanocomposite electrolytes in practical ASS batteries will be considered, by discussing all the ASS batteries based on nanostructured and nanocomposite metal hydrides that have so far been reported. To start, the performance of ASS batteries based on pure and partially ion substituted $LiBH_4$ nanocomposites is reviewed. Next, the implementation of nanostructured $Li_2B_{12}H_{12}$ and other *closo*-(car)borates in practical batteries will be considered. For a complete overview of all metal hydride-based all-solid-state batteries the reader is referred to two excellent reviews on this topic by Latroche et al. and Duchêne et al. [27,123].

4.1. Application of borohydride/oxide nanocomposites in ASS batteries

Over the past years, pure $LiBH_4$ has been studied as a solid electrolyte in several ASS batteries typically using TiS_2 or sulfur as cathode materials [123]. Due to the necessity of a sufficiently high Li-ion conductivity, these ASS batteries operate at a temperature of about 120 °C to ensure the electrolyte remains in the conductive hexagonal polymorph [124]. Since $LiBH_4$ forms a stable interface in contact with metallic lithium, it can be incorporated in a battery using lithium metal as anode, greatly enhancing the energy storage capacity [54]. The attractive mechanical properties (softness) of $LiBH_4$ (similar to most complex hydrides) leads to good interfacial contact with metallic Li anode. On the other hand, the electrochemical stability window of macrocrystalline $LiBH_4$ has been recently determined to be about 2.0 – 2.2 V versus Li^+/Li [26,82]. While this value is close to the working potential of the high-capacity cathode material sulfur, the application of high-voltage cathodes, such as $LiCoO_2$, will be challenging since these operate at a higher working potential and would, therefore, lead to the decomposition of the electrolyte.

In 2016, Das et al. implemented nanoconfined $LiBH_4$ in an ASS lithium-sulfur battery, operating at moderate temperature, i.e. 55 °C [125]. The battery was based on $LiBH_4$ confined in mesoporous silica (MCM-41) as electrolyte. The electrolyte demonstrated promising properties for battery operation, including a room temperature conductivity of 0.1 □ 10^{-3} S cm^{-1}, a cationic transport number of 0.96 and an excellent stability against metallic lithium. The studied Li|-$LiBH_4/SiO_2$|S-C battery was cycled for 40 cycles, at 0.03 C-rate and a working upper and lower cut-off voltage of 3.5 and 1.0 V versus Li^+/Li, respectively (Fig. 12a). From the third cycle onwards the coulombic efficiency was typically 99.6% (Fig. 12b), demonstrating the good cycling stability of the battery. After 40 cycles, the battery delivered a high capacity versus sulfur mass of typically 1220 mAh g^{-1}, 73% of the theoretical sulfur capacity (1675 mAh g^{-1}). Notably, during the first discharge, the cell exhibits a much larger capacity than the theoretical capacity as expected from the amount of sulfur in the cathode. This is most likely related to electrochemical reaction of $LiBH_4$ with the sulfur-based cathode materials, forming a solid electrolyte interphase (SEI) layer.

A similar battery performance was reported by Lefevr et al., who successfully applied ball milled $LiBH_4/SiO_2$ composite electrolytes in

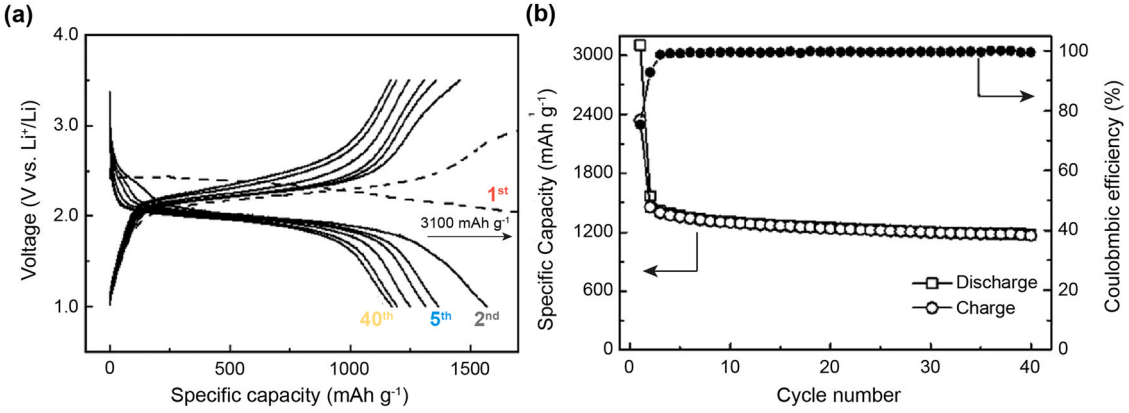

Fig. 12. (a) Discharge-charge profiles of a Li|$LiBH_4/SiO_2$|S-C cell operating at 55 °C with a C-rate of C/30. (b) Specific capacity and Coulombic efficiency as a function of cycle number for the same cell [125].

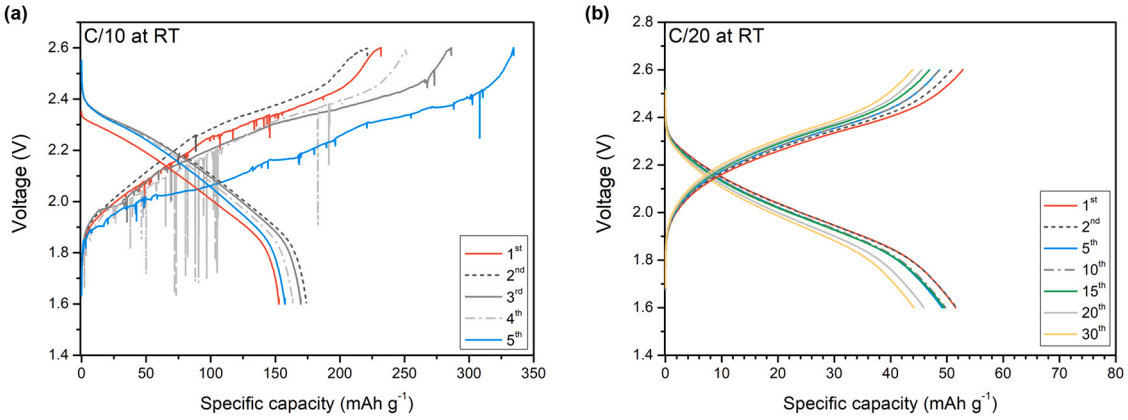

Fig. 13. Discharge-charge profiles of Li|$LiBH_4$/MgO|TiS_2 cells, (a) operating at room temperature with a C-rate of C/10 without any prior heat treatment or cycling experiments and (b) operating at room temperature with a C-rate of C/20 after charging and discharging for 65 cycles at 60 °C with a rate of C/20. Copyright 2020 American Chemical Society. Data has been adapted with permission from ref [126].

ASS Li-S batteries [107]. After 10 discharge-charge cycles at 55 °C with a 0.03 C-rate, the batteries showed a reasonable capacity retention of 794 mAh g^{-1} sulfur with a Coulombic efficiency of 89% and an average capacity loss of 7.2% during the first 10 cycles. In accordance with the results of Das et al. the initial discharge capacity was more than double the theoretical capacity indicating the formation of an SEI layer. While it seems that the formed SEI layer does not limit the following charge-discharge cycles, more work is needed to determine the exact origin of high initial discharge capacity as well as the capacity fading during cycling.

Recently, an ASS battery working at room temperature using $LiBH_4$-based electrolytes was demonstrated for the first time by Gulino et al. [126]. In this work, a nanocomposite electrolyte was prepared by ball milling $LiBH_4$ with MgO nanoparticles, and subsequently incorporated in a Li-TiS_2 battery. Initial cycling of a Li|$LiBH_4$/MgO|TiS_2 battery at room temperature resulted in cell failure after only five cycles (Fig. 13a). In the charge profiles spikes can be observed, that are attributed to inhomogenous Li plating which may be caused by a current density that exceeds the so-called critical current density. Additionally, the authors speculated that in this case only a small SEI layer is formed due to slow kinetics at room temperature. Interestingly, by conditioning the battery at 60 °C prior to operation, it was possible to charge and discharge the battery in a stable manner for 30 cycles at room temperature. Notably, during the application of several charge/discharge cycles at 60 °C, a stable SEI layer forms. While the SEI formation caused an initial increase in contact resistance, it also limited further decomposition of the composite electrolyte. Surprisingly, thereafter it was possible to cycle the battery at room temperature for up to 30 cycles with a specific capacity of about 50 mAh g^{-1} and a capacity retention of about 80% after the 30 cycles (Fig. 13b). Note that the cycling profile is different and specific capacity is lower compared to the cell that was operated without prior conditioning, because this cell was already charged and discharged for 65 cycles at 60 °C, during which the capacity faded. It will be interesting to study whether this remarkable strategy is also applicable to other ASS batteries based metal hydride electrolytes, thereby facilate room temperature operation for other systems as well.

Besides $LiBH_4$/oxide nanocomposites, partially ion-substituted $LiBH_4$/oxide nanocomposites are also promising candidates for application in all-solid-state batteries. In two recent studies, Lu et al. and Yang et al. demonstrated that both LiI- and $LiNH_2$-substituted $LiBH_4$/SiO_2 are indeed attractive electrolytes for next-generation all-solid-state Li-ion batteries [112,120]. In their study, Lu et al. determined that $Li_4(BH_4)_3I$/SiO_2 exhibits a wide apparent electrochemical stability window up to 5 V vs Li^+/Li and a superior Li dendrite suppression capability due to the formation of stable interphase layers. The nanocomposite electrolyte is implemented in ASS batteries based on a sulfur cathode and two different oxide cathodes ($Li_4Ti_5O_{12}$ and $LiCoO_2$), which were successfully operated for three cycles at a 0.05 C-rate and 55 °C. Both the sulfur and $Li_4Ti_5O_{12}$ cathodes required an addition of carbon, respectively, 10 and 15 wt% to the cathode mixture, to induce sufficient electronic conduction.

Similarly, Yang et al. cycled a Li|$Li_2(BH_4)$..(etc.) cell, with excellent specific capacity of 150 mAh g^{-1} and a Coulombic efficiency of 96% after 55 cycles [120]. In both studies, the cycling behavior during the initial charging processes indicate a side reaction between the electrolyte and cathode to form a protective SEI that minimizes further decomposition at excessive potentials. Note that the batteries have only been studied at moderate temperature (55 °C) and it would be interesting to examine their performance at room temperature after formation of the SEI layer. Also interesting is that the presence of the metal oxides in the nanocomposite electrolytes did not compromise the mechanical properties of the electrolytes, hence their good interfacial contact with electrode materials.

4.2. Application of nanostructured closo-borates in ASS batteries

Several reports on the implementation of lithium- and sodium *closo*-(car)borate electrolytes in all-solid-state batteries have been published in the past few years, including an extensive review by Duchêne et al. [27] Most of these batteries are based on partially ion substituted *closo*-borate compounds, such as $Na_2(B_{12}H_{12})_{0.5}(B_{10}H_{10})_{05}$ [25], $Na_4(CB_{11}H_{12})_2(B_{12}H_{12})$ [127] and $Li_2(CB_9H_{10})(CB_{11}H_{12})$ [83], while only few report exist on the implementation of nanostructured *closo*-borates, and no studies have been published yet on the application of interface engineered *closo*-borates in ASS batteries.

Both Kim et al. and Teprovich et al. show that nanostructured $Li_2B_{12}H_{12}$ outperforms macrocrystalline $Li_2B_{12}H_{12}$ as solid electrolyte in ASS Li batteries [91,101]. In Fig. 14, the discharge-charge curves of an all-solid-state Li-TiS_2 battery based on ball-milled $Li_2B_{12}H_{12}$ are depicted, during cycling in the voltage range of 1.6 – 2.7 V vs Li^+/Li at 80 °C and 0.05 C. The battery exhibits an initial discharge capacity of 228 mAh g^{-1} and a good capacity retention over 20 cycles [91]. The battery performs better compared to a similar cell prepared with pristine $Li_2B_{12}H_{12}$ as the solid electrolyte, which delivered a smaller capacity that faded more rapidly during cycling [69]. In addition, the performance of nanostructured $Li_2B_{12}H_{12}$ in a Li-$LiCoO_2$ battery was examined [101]. Cycling of the Li-$LiCoO_2$ cell was performed at moderate temperature (50 °C) between 3.0 V and 4.2 V at a rate of

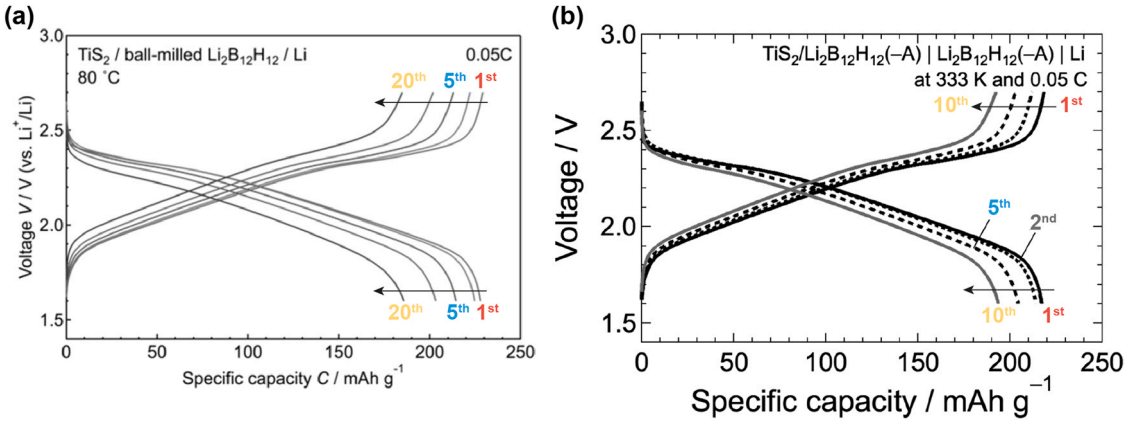

Fig. 14. Discharge-charge profiles of all-solid-state Li|$Li_2B_{12}H_{12}$|TiS_2 battery cells cycled with a C-rate of C/20, based on (a) ball milled $Li_2B_{12}H_{12}$ [91] and (b) pristine $Li_2B_{12}H_{12}$ [69].

0.2 C. The battery exhibited an initial discharge capacity of 63 mAh g^{-1}, which dropped to 37 mAh g^{-1} over 20 charge-discharge cycles (59% capacity retention). Although the capacity for this battery is far below the theoretical capacity (274 mAh g^{-1}), it does demonstrate that nanostructured $Li_2B_{12}H_{12}$ can be incorporated into full battery cells utilizing both sulfur and oxide-based cathode materials.

Unfortunately, to the best of our knowledge no other studies on the implementation of nanostructured *closo*-(car)borates and *closo*-(car)borate/oxide nanocomposites in practical ASS batteries have been published. On the other hand, work on pristine *closo*-(car)borates, including $LiCB_{11}H_{12}$ and $NaCB_{11}H_{12}$ [70], does reveal that these materials can be cycled in ASS batteries working at moderate temperatures even without modifications. As discussed in Sections 3.1.2 and 3.2.2, for a broad class of *closo*-borate and *closo*-carborate materials, higher conductivities can be achieved at ambient temperatures via nanostructuring (ball milling) and nanocomposite formation. Based on these findings, nanostructured or interface engineered *closo*-borates and *closo*-carborates are very promising candidates for ASS metal hydride batteries operating at moderate to low temperatures. It would, therefore, be interesting to investigate their performance in practical ASS batteries and compare it to other metal hydride-based solid ion conductors, as well as sulfide- and oxide-based electrolytes.

For metal hydride- and *closo*-carborate-based ASS batteries, improved safety and a higher energy density compared to today's Li-ion batteries are important properties to keep in mind as well. Besides optimizing their ionic conductivity, it will also be essential to evaluate the thermal, chemical and electrochemical stability of complex hydride electrolytes [128]. For most (pristine) complex metal hydrides, the thermal stability and (electro)chemical stability has been evaluated. Notably, $LiBH_4$ and $NaBH_4$ decompose at 370 °C and 534 °C in the presence of 1 bar hydrogen and thermal decomposition of *closo*-borates typically occurs between 350 °C and 600 °C [27]. The thermal stability of *closo*-carborates has not yet been investigated in detail, but calorimetry measurements indicate that these compounds are thermally stable up to at least 200 °C [129]. Moreover, DFT calculations on the electrochemical stability showed that M$(BH_4)_x$ compounds tend to be oxidized at 2 V vs. Li/Li^+ (Na/Na^+), while *closo*-borate compounds typically have a higher oxidative stability, up to 4 V vs. Li/Li^+ (Na/Na^+) [28]. Unfortunately, the effect of nanostructuring or nanocomposite formation on the thermal and (electro)chemical stability of complex metal hydrides has not yet been studied systematically. The decomposition pathways, and thereby stability, might be affected by nanostructuring and nanocomposite formation. Hence, experimental stability studies could give valuable information for the application of modified metal hydrides in ASS batteries.

5. Conclusion and perspectives

Complex metal hydrides are a promising class of materials for a variety of energy storage applications, including as solid-state ion conductors for all-solid-state batteries. In the past decade, large efforts have been made to improve the electrochemical performance of complex hydride-based electrolytes, specifically their ionic conductivity at room temperature. Nanostructuring and nanocomposite formation are intriguing strategies that offer a great potential to improve the ion mobility in metal hydride ion conductors.

The design and fabrication of nanostructured and interface engineered metal hydride-based solid electrolytes has been discussed in this review. Via nanostructuring by ball-milling, conductive high-temperature polymorphs remain present when cooled to ambient temperature for a wide range of compounds, such as $LiBH_4$, $Li_2B_{12}H_{12}$ and $NaCB_{11}H_{12}$. Unfortunately, these nanostructured polymorphs are not thermally stable, and their conductivities degrade when cycled at high temperatures or over a long time. Therefore, it is important to find ways to preserve the conductivity of nanostructured materials. More stable compounds are obtained by forming nanocomposites through melt infiltration or ball milling of metal hydrides with metal oxides. The conductivity of metal hydride/metal oxide nanocomposites, for example based on $LiBH_4$, $Li_2(BH_4)(NH_2)$ and $NaCB_{11}H_{12}$, is greatly enhanced and remains stable upon cycling, even at high temperatures. However, several studies demonstrate that sufficient interface interaction between the metal hydride and the insulating scaffold is critical for the success of this approach. Hence, in future work, interface interactions at the hydride-oxide interface should be studied further to determine the exact nature of these interactions and the effects of the chemical and physical (e.g. pore structure and morphology) properties of the oxides on nanocomposite conductivity.

Furthermore, the application of nanostructured and interface engineered metal hydride-based electrolytes in all-solid-state batteries is still in an early stage of development. Further works are needed to gain more insight on the performance of ASS batteries based on metal hydride electrolytes. While some promising examples of complex hydride-based ASS batteries have been shown, unfavourable side reactions and capacity fading are still critical issues that should be addressed. Fundamental research that addresses the origin of capacity fading, the formation of (stable) interface layers and the compatibility with high-voltage cathodes will be essential for the application of metal hydride ion conductors in ASS batteries. Additionally, studies on the long-term (thermal and (electro)chemical) stability and dendrite formation, as well as practical aspects including manufacturing costs, optimized (gravimetric and volumetric) energy density and battery recycling are

highly relevant. Here, it should be considered that the incorporation of an oxide, which often have a high density, in a metal hydride-based ion conductor heavily influences the theoretical energy density of a metal hydride-based ASS battery. For example, the gravimetric energy density of a Li|$LiBH_4$/MgO|TiS_2 battery is about 35% of the expected energy density of a Li|$LiBH_4$|TiS_2 cell considering the same volume of all battery components. On the other hand, the battery manufacturing cost might be lowered due to the incorporation of inexpensive oxide scaffolds, thereby reducing the amount of complex metal hydride needed for the battery. We hope that this review can stimulate extensive and insightful studies for the design of novel metal hydride/oxide nanocomposites with excellent electrochemical performances for next generation batteries.

CRediT authorship contribution statement

Laura de Kort: Writing – original draft, reviewing and editing. **Valerio Gulino:** Writing, reviewing and editing. **Petra de Jongh:** Supervision, editing and reviewing. **Peter Ngene:** Conceptualization, Supervision, Writing – reviewing and editing.

Declaration of Competing Interest

The authors declare that they have no known competing financial interests or personal relationships that could have appeared to influence the work reported in this paper.

Acknowledgements

The authors greatly appreciate funding from the The Dutch Research Council NWO (Nederlandse Organisatie voor Wetenschappelijk Onderzoek) Materials for sustainability Mat4Sus) (739.017.009) grant, as well as the NWO ECHO (712.015.005) grant.

References

[1] D.L. McCollum, W. Zhou, C. Bertram, H.S. De Boer, V. Bosetti, S. Busch, J. Després, L. Drouet, J. Emmerling, M. Fay, O. Fricko, S. Fujimori, M. Gidden, M. Harmsen, D. Huppmann, G. Iyer, V. Krey, E. Kriegler, C. Nicolas, S. Pachauri, S. Parkinson, M. Poblete-Cazenave, P. Rafaj, N. Rao, J. Rozenberg, A. Schmitz, W. Schoepp, D. Van Vuuren, K. Riahi, Energy investment needs for fulfilling the Paris agreement and achieving the sustainable development goals, Nat. Energy 3 (2018) 589–599, https://doi.org/10.1038/s41560-018-0179-z

[2] D. Larcher, J.M. Tarascon, Towards greener and more sustainable batteries for electrical energy storage, Nat. Chem. 7 (2015) 19–29, https://doi.org/10.1038/nchem.2085

[3] B. Dunn, H. Kamath, J.M. Tarascon, Electrical energy storage for the grid: a battery of choices, Science 334 (80) (2011) 928–935, https://doi.org/10.1126/science.1212741

[4] J.M. Tarascon, M. Armand, Issues and challenges facing rechargeable lithium batteries, Nature 414 (2001) 359–367, https://doi.org/10.1038/35104644

[5] J.B. Goodenough, K.S. Park, The Li-ion rechargeable battery: a perspective, J. Am. Chem. Soc. 135 (2013) 1167–1176, https://doi.org/10.1021/ja3091438

[6] J. Janek, W.G. Zeier, A solid future for battery development, Nat. Energy 1 (2016) 1–4, https://doi.org/10.1038/nenergy.2016.141

[7] A. Manthiram, X. Yu, S. Wang, Lithium battery chemistries enabled by solid-state electrolytes, Nat. Rev. Mater. 2 (2017) 1–16, https://doi.org/10.1038/natrevmats.2016.103

[8] J. Li, C. Ma, M. Chi, C. Liang, N.J. Dudney, Solid electrolyte: the key for high-voltage lithium batteries, Adv. Energy Mater. 5 (2015) 1–6, https://doi.org/10.1002/aenm.201401408

[9] K. Takada, Progress in solid electrolytes toward realizing solid-state lithium batteries, J. Power Sources 394 (2018) 74–85, https://doi.org/10.1016/j.jpowsour.2018.05.003

[10] J.G. Kim, B. Son, S. Mukherjee, N. Schuppert, A. Bates, O. Kwon, M.J. Choi, H.Y. Chung, S. Park, A review of lithium and non-lithium based solid state batteries, J. Power Sources 282 (2015) 299–322, https://doi.org/10.1016/j.jpowsour.2015.02.054

[11] K. Takada, Progress and prospective of solid-state lithium batteries, Acta Mater. 61 (2013) 759–770, https://doi.org/10.1016/j.actamat.2012.10.034

[12] J.C. Bachman, S. Muy, A. Grimaud, H.H. Chang, N. Pour, S.F. Lux, O. Paschos, F. Maglia, S. Lupart, P. Lamp, L. Giordano, Y. Shao-Horn, Inorganic solid-state electrolytes for lithium batteries: mechanisms and properties governing ion conduction, Chem. Rev. 116 (2016) 140–162, https://doi.org/10.1021/acs.chemrev.5b00563

[13] N. Boaretto, I. Garbayo, S. Valiyaveettil-SobhanRaj, A. Quintela, C. Li, M. Casas-Cabanas, F. Aguesse, Lithium solid-state batteries: state-of-the-art and challenges for materials, interfaces and processing, J. Power Sources 502 (2021) 229919, https://doi.org/10.1016/j.jpowsour.2021.229919

[14] E. Rangasamy, Z. Liu, M. Gobet, K. Pilar, G. Sahu, W. Zhou, H. Wu, S. Greenbaum, C. Liang, iodide-Based Li7P2S8I superionic Conduct., J. Am. Chem. Soc. 137 (2015) 1384–1387, https://doi.org/10.1021/ja508723m

[15] Y. Seino, T. Ota, K. Takada, A. Hayashi, M. Tatsumisago, A sulphide lithium super ion conductor is superior to liquid ion conductors for use in rechargeable batteries, Energy Environ. Sci. 7 (2014) 627–631, https://doi.org/10.1039/c3ee41655k

[16] V. Thangadurai, W. Weppner, Recent progress in solid oxide and lithium ion conducting electrolytes research, Ionics 12 (2006) 81–92, https://doi.org/10.1007/s11581-006-0013-7

[17] M. Itoh, Y. Inaguma, W.H. Jung, L. Chen, T. Nakamura, High lithium ion conductivity in the perovskite-type compounds $Ln_{12}Li_{12}TiO_3$(Ln=La,Pr,Nd,Sm), Solid State Ion. 70–71 (1994) 203–207, https://doi.org/10.1016/0167-2738(94)90310-7

[18] S. Stramare, V. Thangadurai, W. Weppner, Lithium lanthanum titanates: a review, Chem. Mater. 15 (2003) 3974–3990, https://doi.org/10.1021/cm0300516

[19] M. Matsuo, Y. Nakamori, S.I. Orimo, H. Maekawa, H. Takamura, Lithium superionic conduction in lithium borohydride accompanied by structural transition, Appl. Phys. Lett. 91 (2007) 2–5, https://doi.org/10.1063/1.2817934

[20] N. Verdal, T.J. Udovic, V. Stavila, W.S. Tang, J.J. Rush, A.V. Skripov, Anion reorientations in the superionic conducting phase of $Na_2B_{12}H_{12}$, J. Phys. Chem. C. 118 (2014) 17483–17489, https://doi.org/10.1021/jp506252c

[21] W.S. Tang, M. Matsuo, H. Wu, V. Stavila, W. Zhou, A.A. Talin, A.V. Soloninin, R.V. Skoryunov, O.A. Babanova, A.V. Skripov, A. Unemoto, S.I. Orimo, T.J. Udovic, Liquid-like ionic conduction in solid lithium and sodium monocarba-closo-decaborates near or at room temperature, Adv. Energy Mater. 6 (2016) 1–6, https://doi.org/10.1002/aenm.201502237

[22] A. Remhof, Z. Łodziana, F. Buchter, P. Martelli, F. Pendolino, O. Friedrichs, A. Züttel, J.P. Embs, Rotational diffusion in $NaBH_4$, J. Phys. Chem. C. 113 (2009) 16834–16837, https://doi.org/10.1021/jp906174e

[23] S. Kim, H. Oguchi, N. Toyama, T. Sato, S. Takagi, T. Otomo, D. Arunkumar, N. Kuwata, J. Kawamura, S. ichi Orimo, A complex hydride lithium superionic conductor for high-energy-density all-solid-state lithium metal batteries, Nat. Commun. 10 (2019) 1081, https://doi.org/10.1038/s41467-019-09061-9

[24] L. Duchêne, R.S. Kühnel, D. Rentsch, A. Remhof, H. Hagemann, C. Battaglia, A highly stable sodium solid-state electrolyte based on a dodeca/deca-borate equimolar mixture, Chem. Commun. 53 (2017) 4195–4198, https://doi.org/10.1039/c7cc00794a

[25] L. Duchêne, R.S. Kühnel, E. Stilp, E. Cuervo Reyes, A. Remhof, H. Hagemann, C. Battaglia, A stable 3 v all-solid-state sodium-ion battery based on a closoborate electrolyte, Energy Environ. Sci. 10 (2017) 2609–2615, https://doi.org/10.1039/c7ee02420g

[26] R. Asakura, L. Duchêne, R.S. Kühnel, A. Remhof, H. Hagemann, C. Battaglia, Electrochemical oxidative stability of hydroborate-based solid-state electrolytes, ACS Appl. Energy Mater. 2 (2019) 6924–6930, https://doi.org/10.1021/acsaem.9b01487

[27] L. Duchêne, A. Remhof, H. Hagemann, C. Battaglia, Status and prospects of hydroborate electrolytes for all-solid-state batteries, Energy Storage Mater. 25 (2020) 782–794, https://doi.org/10.1016/j.ensm.2019.08.032

[28] Z. Lu, F. Ciucci, Metal borohydrides as electrolytes for solid-state Li, Na, Mg, and Ca batteries: a first-principles study, Chem. Mater. 29 (2017) 9308–9319, https://doi.org/10.1021/acs.chemmater.7b03284

[29] M. Matsuo, H. Takamura, H. Maekawa, H.W. Li, S.I. Orimo, Stabilization of lithium superionic conduction phase and enhancement of conductivity of $LiBH_4$ by LiCl addition, Appl. Phys. Lett. 94 (2009) 2–5, https://doi.org/10.1063/1.3088857

[30] H. Maekawa, M. Matsuo, H. Takamura, M. Ando, Y. Noda, Halide-stabilized $LiBH_4$, a room-temperature lithium fast-ion conductor, J. Am. Chem. Soc. 131 (2009) 894–895.

[31] L.H. Rude, E. Groppo, L.M. Arnbjerg, D.B. Ravnsbæk, R.A. Malmkjær, Y. Filinchuk, M. Baricco, F. Besenbacher, T.R. Jensen, Iodide substitution in lithium borohydride, $LiBH_4$-LiI, J. Alloy. Compd. 509 (2011) 8299–8305, https://doi.org/10.1016/j.jallcom.2011.05.031

[32] T. Mezaki, Y. Kuronuma, I. Oikawa, A. Kamegawa, H. Takamura, Li-ion conductivity and phase stability of Ca-doped LiBH4 under high pressure, Inorg. Chem. 55 (2016) 10484–10489, https://doi.org/10.1021/acs.inorgchem.6b01678

[33] Z. Yao, S. Kim, K. Michel, Y. Zhang, M. Aykol, C. Wolverton, Stability and conductivity of cation- and anion-substituted $LiBH_4$-based solid-state electrolytes, Phys. Rev. Mater. 2 (2018) 37–39, https://doi.org/10.1103/PhysRevMaterials.2.065402

[34] M. Paskevicius, L.H. Jepsen, P. Schouwink, R. Černý, D.B. Ravnsbæk, Y. Filinchuk, M. Dornheim, F. Besenbacher, T.R. Jensen, Metal borohydrides and derivatives-synthesis, structure and properties, Chem. Soc. Rev. 46 (2017) 1565–1634, https://doi.org/10.1039/c6cs00705h

[35] P. Heitjans, E. Tobschall, M. Wilkening, Ion transport and diffusion in nanocrystalline and glassy ceramics, Eur. Phys. J. Spec. Top. 161 (2008) 97–108, https://doi.org/10.1140/epjst/e2008-00753-4

[36] V. Epp, M. Wilkening, Motion of Li^+ in nanoengineered $LiBH_4$ and $LiBH_4$:Al_2O_3 comparison with the microcrystalline form, ChemPhysChem 14 (2013) 3706–3713, https://doi.org/10.1002/cphc.201300743

[37] W.S. Tang, M. Matsuo, H. Wu, V. Stavila, A. Unemoto, S.I. Orimo, T.J. Udovic, Stabilizing lithium and sodium fast-ion conduction in solid polyhedral-borate salts at device-relevant temperatures, Energy Storage Mater. 4 (2016) 79–83, https://doi.org/10.1016/j.ensm.2016.03.004

[38] Z. Zou, Y. Li, Z. Lu, D. Wang, Y. Cui, B. Guo, Y. Li, X. Liang, J. Feng, H. Li, C.W. Nan, M. Armand, L. Chen, K. Xu, S. Shi, Mobile ions in composite solids, Chem. Rev. 120 (2020) 4169–4221, https://doi.org/10.1021/acs.chemrev.9b00760

[39] P.E. De Jongh, P. Adelhelm, Nanosizing and nanoconfinement: New strategies towards meeting hydrogen storage goals, ChemSusChem 3 (2010) 1332–1348, https://doi.org/10.1002/cssc.201000248

[40] C.C. Liang, Conduction characteristics of the lithium iodide-aluminum oxide solid electrolytes, J. Electrochem. Soc. 120 (1973) 1289, https://doi.org/10.1149/1.2403248

[41] L.J. Bannenberg, M. Heere, H. Benzidi, J. Montero, E.M. Dematteis, S. Suwarno, T. Jaroń, M. Winny, P.A. Orłowski, W. Wegner, A. Starobrat, K.J. Fijałkowski, W. Grochala, Z. Qian, J.P. Bonnet, I. Nuta, W. Lohstroh, C. Zlotea, O. Mounkachi, F. Cuevas, C. Chatillon, M. Latroche, M. Fichtner, M. Baricco, B.C. Hauback, A. El Kharbachi, Metal (boro-) hydrides for high energy density storage and relevant emerging technologies, Int. J. Hydrog. Energy 45 (2020) 33687–33730, https://doi.org/10.1016/j.ijhydene.2020.08.119

[42] P.E. de Jongh, D. Blanchard, M. Matsuo, T.J. Udovic, S. Orimo, Complex hydrides as room-temperature solid electrolytes for rechargeable batteries, Appl. Phys. A Mater. Sci. Process. 122 (2016) 1–6, https://doi.org/10.1007/s00339-016-9807-2

[43] R. Mohtadi, S.I. Orimo, The renaissance of hydrides as energy materials, Nat. Rev. Mater. 2 (2016) 1–16, https://doi.org/10.1038/natrevmats.2016.91

[44] M. Hirscher, V.A. Yartys, M. Baricco, J. Bellosta von Colbe, D. Blanchard, R.C. Bowman, D.P. Broom, C.E. Buckley, F. Chang, P. Chen, Y.W. Cho, J.C. Crivello, F. Cuevas, W.I.F. David, P.E. de Jongh, R.V. Denys, M. Dornheim, M. Felderhoff, Y. Filinchuk, G.E. Froudakis, D.M. Grant, E.M.A. Gray, B.C. Hauback, T. He, T.D. Humphries, T.R. Jensen, S. Kim, Y. Kojima, M. Latroche, H.W. Li, M.V. Lototskyy, J.W. Makepeace, K.T. Møller, L. Naheed, P. Ngene, D. Noréus, M.M. Nygård, S. ichi Orimo, M. Paskevicius, L. Pasquini, D.B. Ravnsbæk, M. Veronica Sofianos, T.J. Udovic, T. Vegge, G.S. Walker, C.J. Webb, C. Weidenthaler, C. Zlotea, Materials for hydrogen-based energy storage – past, recent progress and future outlook, J. Alloy. Compd. 827 (2020) 153548, https://doi.org/10.1016/j.jallcom.2019.153548

[45] O. Zavorotynska, I. Saldan, S. Hino, T.D. Humphries, S. Deledda, B.C. Hauback, Hydrogen cycling in γ-$Mg(BH_4)_2$ with cobalt-based additives, J. Mater. Chem. A. 3 (2015) 6592–6602, https://doi.org/10.1039/c5ta00511f

[46] B. Bogdanović, M. Schwickardi, Ti-doped alkali metal aluminium hydrides as potential novel reversible hydrogen storage materials, J. Alloy. Compd. 253–254 (1997) 1–9, https://doi.org/10.1016/S0925-8388(96)03049-6

[47] K. Manickam, P. Mistry, G. Walker, D. Grant, C.E. Buckley, T.D. Humphries, M. Paskevicius, T. Jensen, R. Albert, K. Peinecke, M. Felderhoff, Future perspectives of thermal energy storage with metal hydrides, Int. J. Hydrog. Energy 44 (2019) 7738–7745, https://doi.org/10.1016/j.ijhydene.2018.12.011

[48] V. Gulino, A. Wolczyk, A.A. Golov, R.A. Eremin, M. Palumbo, C. Nervi, V.A. Blatov, D.M. Proserpio, M. Baricco, Combined DFT and geometrical-topological analysis of Li-ion conductivity in complex hydrides, Inorg. Chem. Front. 7 (2020) 3115–3125, https://doi.org/10.1039/d0qi00577k

[49] M. Matsuo, S.I. Orimo, Lithium fast-ionic conduction in complex hydrides: review and prospects, Adv. Energy Mater. 1 (2011) 161–172, https://doi.org/10.1002/aenm.201000012

[50] T. Ikeshoji, E. Tsuchida, T. Morishita, K. Ikeda, M. Matsuo, Y. Kawazoe, S.I. Orimo, Fast-ionic conductivity of Li^+ in $LiBH_4$, Phys. Rev. B - Condens. Matter Mater. Phys. 83 (2011) 1–5, https://doi.org/10.1103/PhysRevB.83.144301

[51] J.S.G. Myrdal, D. Blanchard, D. Sveinbjörnsson, T. Vegge, Li-ion conduction in the LiBH4:LiI system from density functional theory calculations and quasi-elastic neutron scattering, J. Phys. Chem. C. 117 (2013) 9084–9091, https://doi.org/10.1021/jp311980h

[52] N. Verdal, T.J. Udovic, J.J. Rush, The nature of BH_4^- reorientations in hexagonal $LiBH_4$, J. Phys. Chem. C. 116 (2012) 1614–1618, https://doi.org/10.1021/jp211754g

[53] Y.S. Lee, Y.W. Cho, Fast lithium ion migration in room temperature $LiBH_4$, J. Phys. Chem. C. 121 (2017) 17773–17779, https://doi.org/10.1021/acs.jpcc.7b06328

[54] K. Kisu, S. Kim, H. Oguchi, N. Toyama, S. ichi Orimo, Interfacial stability between $LiBH_4$-based complex hydride solid electrolytes and Li metal anode for all-solid-state Li batteries, J. Power Sources 436 (2019) 226821, https://doi.org/10.1016/j.jpowsour.2019.226821

[55] H. Oguchi, M. Matsuo, T. Sato, H. Takamura, H. Maekawa, H. Kuwano, S. Orimo, Lithium-ion conduction in complex hydrides $LiAlH_4$ and Li_3AlH_6, J. Appl. Phys. 107 (2010) 105–108, https://doi.org/10.1063/1.3356981

[56] H. Oguchi, M. Matsuo, S. Kuromoto, H. Kuwano, S. Orimo, Sodium-ion conduction in complex hydrides $NaAlH_4$ and Na_3AlH_6, J. Appl. Phys. 111 (2012) 4–7, https://doi.org/10.1063/1.3681362

[57] M. Matsuo, H. Oguchi, T. Sato, H. Takamura, E. Tsuchida, T. Ikeshoji, S.I. Orimo, Sodium and magnesium ionic conduction in complex hydrides, J. Alloy. Compd. 580 (2013) S98–S101, https://doi.org/10.1016/j.jallcom.2013.01.058

[58] B.A. Boukamp, R.A. Huggins, Ionic conductivity in lithium imide, Phys. Lett. A 72 (1979) 464–466, https://doi.org/10.1016/0375-9601(79)90846-6

[59] X. Luo, A. Rawal, K.F. Aguey-Zinsou, Investigating the factors affecting the ionic conduction in nanoconfined $NaBH_4$, Inorganics 9 (2021) 1–10, https://doi.org/10.3390/inorganics9010002

[60] B. Paik, A. Wolczyk, Lithium Imide (Li_2NH) as a solid-state electrolyte for electrochemical energy storage applications, J. Phys. Chem. C. 123 (2019) 1619–1625, https://doi.org/10.1021/acs.jpcc.8b10528

[61] B. Paik, M. Matsuo, T. Sato, L. Qu, A.R. Wolczyk, S.I. Orimo, Effect of the structural evolution on the ionic conductivity of Li-N-H system during the dehydrogenation, Appl. Phys. Lett. 108 (2016) 213903, https://doi.org/10.1063/1.4952601

[62] W. Li, G. Wu, Z. Xiong, Y.P. Feng, P. Chen, Li^+ ionic conductivities and diffusion mechanisms in Li-based imides and lithium amide, Phys. Chem. Chem. Phys. 14 (2012) 1596–1606, https://doi.org/10.1039/c2cp23636b

[63] Y. Yan, J.B. Grinderslev, M. Jørgensen, L.N. Skov, J. rgen Skibsted, T.R. Jensen, Ammine magnesium borohydride nanocomposites for all-solid-state magnesium batteries, ACS Appl. Energy Mater. 3 (2020) 9264–9270, https://doi.org/10.1021/acsaem.0c01599

[64] N. Verdal, J.H. Her, V. Stavila, A.V. Soloninin, O.A. Babanova, A.V. Skripov, T.J. Udovic, J.J. Rush, Complex high-temperature phase transitions in $Li_2B_{12}H_{12}$ and $Na_2B_{12}H_{12}$, J. Solid State Chem. 212 (2014) 81–91, https://doi.org/10.1016/j.jssc.2014.01.006

[65] T.J. Udovic, M. Matsuo, A. Unemoto, N. Verdal, V. Stavila, A.V. Skripov, J.J. Rush, H. Takamura, S. Orimo, Sodium superionic conduction in $Na_2B_{12}H_{12}$, Chem. Commun. 50 (2014) 3750–3752, https://doi.org/10.1039/C3CC49805K

[66] A.V. Skripov, O.A. Babanova, A.V. Soloninin, V. Stavila, N. Verdal, T.J. Udovic, J.J. Rush, Nuclear magnetic resonance study of atomic motion in $A_2B_{12}H_{12}$ (A = Na, K, Rb, Cs): anion reorientations and Na^+ mobility, J. Phys. Chem. C. 117 (2013) 25961–25968, https://doi.org/10.1021/jp4106585

[67] A.V. Skripov, A.V. Soloninin, O.A. Babanova, R.V. Skoryunov, Nuclear magnetic resonance studies of atomic motion in borohydride-based materials: fast anion reorientations and cation diffusion, J. Alloy. Compd. 645 (2015) S428–S433, https://doi.org/10.1016/j.jallcom.2014.12.089

[68] L. He, H.W. Li, H. Nakajima, N. Tumanov, Y. Filinchuk, S.J. Hwang, M. Sharma, H. Hagemann, E. Akiba, Synthesis of a bimetallic dodecaborate $LiNaB_{12}H_{12}$ with outstanding superionic conductivity, Chem. Mater. 27 (2015) 5483–5486, https://doi.org/10.1021/acs.chemmater.5b01568

[69] A. Unemoto, K. Yoshida, T. Ikeshoji, S.I. Orimo, Bulk-type all-solid-state lithium batteries using complex hydrides containing cluster-anions, Mater. Trans. 57 (2016) 1639–1644, https://doi.org/10.2320/matertrans.MAW201601

[70] W.S. Tang, A. Unemoto, W. Zhou, V. Stavila, M. Matsuo, H. Wu, S.I. Orimo, T.J. Udovic, Unparalleled lithium and sodium superionic conduction in solid electrolytes with large monovalent cage-like anions, Energy Environ. Sci. 8 (2015) 3637–3645, https://doi.org/10.1039/c5ee02941d

[71] W.S. Tang, M. Dimitrievska, V. Stavila, W. Zhou, H. Wu, A.A. Talin, T.J. Udovic, Order-disorder transitions and superionic conductivity in the sodium nido-undeca(carba)borates, Chem. Mater. 29 (2017) 10496–10509, https://doi.org/10.1021/acs.chemmater.7b04332

[72] Z. Lu, F. Ciucci, Structural origin of the superionic Na conduction in Na2B10H10 closo-borates and enhanced conductivity by Na deficiency for high performance solid electrolytes, J. Mater. Chem. A 4 (2016) 17740–17748, https://doi.org/10.1039/c6ta07443j

[73] K.E. Kweon, J.B. Varley, P. Shea, N. Adelstein, P. Mehta, T.W. Heo, T.J. Udovic, V. Stavila, B.C. Wood, Structural, chemical, and dynamical frustration: origins of superionic conductivity in closo-borate solid electrolytes, Chem. Mater. 29 (2017) 9142–9153, https://doi.org/10.1021/acs.chemmater.7b02902

[74] J.B. Varley, K. Kweon, P. Mehta, P. Shea, T.W. Heo, T.J. Udovic, V. Stavila, B.C. Wood, Understanding ionic conductivity trends in polyborane solid electrolytes from Ab initio molecular dynamics, ACS Energy Lett. 2 (2017) 250–255, https://doi.org/10.1021/acsenergylett.6b00620

[75] T.J. Udovic, M. Matsuo, W.S. Tang, H. Wu, V. Stavila, A.V. Soloninin, R.V. Skoryunov, O.A. Babanova, A.V. Skripov, J.J. Rush, A. Unemoto, H. Takamura, S.I. Orimo, Exceptional superionic conductivity in disordered sodium decahydro-closo-decaborate, Adv. Mater. 26 (2014) 7622–7626, https://doi.org/10.1002/adma.201403157

[76] R. Moury, A. Gigante, H. Hagemann, An alternative approach to the synthesis of NaB_3H_8 and $Na_2B_{12}H_{12}$ for solid electrolyte applications, Int. J. Hydrog. Energy 42 (2017) 22417–22421, https://doi.org/10.1016/j.ijhydene.2017.02.044

[77] A. Gigante, L. Duchêne, R. Moury, M. Pupier, A. Remhof, H. Hagemann, Direct solution-based synthesis of $Na_4(B_{12}H_{12})(B_{10}H_{10})$ solid electrolyte, ChemSusChem 12 (2019) 4832–4837, https://doi.org/10.1002/cssc.201902152

[78] A. Berger, C.E. Buckley, M. Paskevicius, Synthesis of closo-$CB_{11}H_{12}$-salts using common laboratory reagents, Inorg. Chem. (2021), https://doi.org/10.1021/acs.inorgchem.1c01896

[79] Y. Yan, R.S. Kühnel, A. Remhof, L. Duchêne, E.C. Reyes, D. Rentsch, Z. Łodziana, C. Battaglia, A lithium amide-borohydride solid-state electrolyte with lithium-ion conductivities comparable to liquid electrolytes, Adv. Energy Mater. 7 (2017) 1–7, https://doi.org/10.1002/aenm.201700294

[80] R. Miyazaki, T. Karahashi, N. Kumatani, Y. Noda, M. Ando, H. Takamura, M. Matsuo, S. Orimo, H. Maekawa, Room temperature lithium fast-ion conduction and phase relationship of LiI stabilized $LiBH_4$, Solid State Ion. 192 (2011) 143–147, https://doi.org/10.1016/j.ssi.2010.05.017

[81] V. Gulino, E.M. Dematteis, M. Corno, M. Palumbo, M. Baricco, Theoretical and experimental studies of $LiBH_4$-LiBr phase diagram, ACS Appl. Energy Mater. 4 (2021) 7327–7337, https://doi.org/10.1021/acsaem.1c01455

[82] V. Gulino, M. Brighi, E.M. Dematteis, F. Murgia, C. Nervi, R. Černý, M. Baricco, Phase stability and fast ion conductivity in the hexagonal LiBH4-LiBr-LiCl solid solution, Chem. Mater. 31 (2019) 5133–5144, https://doi.org/10.1021/acs.chemmater.9b01035

[83] S. Kim, K. Kisu, S. Takagi, H. Oguchi, S.I. Orimo, Complex hydride solid electrolytes of the $Li(CB_9H_{10})$-$Li(CB_{11}H_{12})$ quasi-binary system: relationship between the solid solution and phase transition, and the electrochemical properties, ACS Appl. Energy Mater. 3 (2020) 4831–4839, https://doi.org/10.1021/acsaem.0c00433

[84] M. Brighi, F. Murgia, Z. Łodziana, P. Schouwink, A. Wołczyk, R. Černý, A mixed anion hydroborate/carba-hydroborate as a room temperature Na-ion solid electrolyte, J. Power Sources 404 (2018) 7–12, https://doi.org/10.1016/j.jpowsour.2018.09.085

[85] D. Bork, P. Heitjans, NMR relaxation study of ion dynamics in nanocrystalline and polycrystalline $LiNbO_3$, J. Phys. Chem. B. 102 (1998) 7303–7306, https://doi.org/10.1021/jp981536y

[86] H. Gleiter, Nanostructured materials: basic concepts and microstructure, Acta Mater. 48 (2000) 1–29, https://doi.org/10.1016/S1359-6454(99)00285-2

[87] P. Heitjans, M. Masoud, A. Feldhoff, M. Wilkening, NMR and impedance studies of nanocrystalline and amorphous ion conductors: Lithium niobate as a model system, Faraday Discuss. 134 (2007) 67–82, https://doi.org/10.1039/b602887j

[88] M. Wilkening, V. Epp, A. Feldhoff, P. Heitjans, Tuning the Li diffusivity of poor ionic conductors by mechanical treatment: high li conductivity of strongly defective $LiTaO_3$ nanoparticles, J. Phys. Chem. C. 112 (2008) 9291–9300, https://doi.org/10.1021/jp801537s

[89] D. Sveinbjörnsson, J.S.G. Myrdal, D. Blanchard, J.J. Bentzen, T. Hirata, M.B. Mogensen, P. Norby, S.I. Orimo, T. Vegge, Effect of heat treatment on the lithium ion conduction of the $LiBH_4$-LiI solid solution, J. Phys. Chem. C. 117 (2013) 3249–3257, https://doi.org/10.1021/jp310050g

[90] Y. Nakagawa, T. Kimura, T. Ohki, S. Isobe, T. Shibayama, Effect of mechanical milling on lithium-ion conductivity of $LiAlH_4$, Solid State Ion. 365 (2021) 115656, https://doi.org/10.1016/j.ssi.2021.115656

[91] S. Kim, N. Toyama, H. Oguchi, T. Sato, S. Takagi, T. Ikeshoji, S.I. Orimo, Fast lithium-ion conduction in atom-deficient closo-type complex hydride solid electrolytes, Chem. Mater. 30 (2018) 386–391, https://doi.org/10.1021/acs.chemmater.7b03986

[92] V. Gulino, L. Barberis, P. Ngene, M. Baricco, P.E. De Jongh, Enhancing Li-ion conductivity in $LiBH_4$-based solid electrolytes by adding various nanosized oxides, ACS Appl. Energy Mater. 3 (2020) 4941–4948, https://doi.org/10.1021/acsaem.9b02268

[93] R.C. Agrawal, R.K. Gupta, Superionic solids: composite electrolyte phase - an overview, J. Mater. Sci. 34 (1999) 1131–1162, https://doi.org/10.1023/A:1004598902146

[94] I. Skobelev, N. Uvarov, E. Hairetdinov, Composite solid electrolytes $MeNO_3$-Al_2O_3 (Me = Li, Na, K), Solid State Ion. 88 (1996) 86–89.

[95] D. Blanchard, A. Nale, D. Sveinbjörnsson, T.M. Eggenhuisen, M.H.W. Verkuijlen, Suwarno, T. Vegge, A.P.M. Kentgens, P.E. De Jongh, Nanoconfined $LiBH_4$ as a fast lithium ion conductor, Adv. Funct. Mater. 25 (2015) 184–192, https://doi.org/10.1002/adfm.201402538

[96] J. Maier, Ionic conduction in space charge regions, Prog. Solid State Chem. 23 (1995) 171–263, https://doi.org/10.1016/0079-6786(95)00004-E

[97] J. Maier, Point-defect thermodynamics and size effects, Solid State Ion. 131 (2000) 13–22, https://doi.org/10.1016/S0167-2738(00)00618-4

[98] P.E. De Jongh, T.M. Eggenhuisen, Nanoporous Materials and Confined Liquids, in: C. de Mello Donegá (Ed.), Nanoparticles Work. Nanosci. Springer Berlin Heidelberg, Berlin, Heidelberg, 2014, pp. 99–120, https://doi.org/10.1007/978-3-662-44823-6_4

[99] Y.S. Choi, Y.S. Lee, D.J. Choi, K.H. Chae, K.H. Oh, Y.W. Cho, Enhanced Li ion conductivity in $LiBH_4$-Al_2O_3 mixture via interface engineering, J. Phys. Chem. C. 121 (2017) 26209–26215, https://doi.org/10.1021/acs.jpcc.7b08862

[100] L.M. De Kort, J. Harmel, P.E. De Jongh, P. Ngene, The effect of nanoscaffold porosity and surface chemistry on the Li-ion conductivity of $LiBH_4$-$LiNH_2$/metal oxide nanocomposites, J. Mater. Chem. A. 8 (2020) 20687–20697, https://doi.org/10.1039/d0ta07600g

[101] J.A. Teprovich, H. Colón-Mercado, A.L. Washington, P.A. Ward, S. Greenway, D.M. Missimer, H. Hartman, J. Velten, J.H. Christian, R. Zidan, Bi-functional $Li_2B_{12}H_{12}$ for energy storage and conversion applications: solid-state electrolyte and luminescent down-conversion dye, J. Mater. Chem. A. 3 (2015) 22853–22859, https://doi.org/10.1039/c5ta06549f

[102] M.H.W. Verkuijlen, P. Ngene, D.W. De Kort, C. Barré, A. Nale, E.R.H. Van Eck, P.J.M. Van Bentum, P.E. De Jongh, A.P.M. Kentgens, Nanoconfined $LiBH_4$ and enhanced mobility of Li^+ and BH_4^- studied by solid-state NMR, J. Phys. Chem. C. 116 (2012) 22169–22178, https://doi.org/10.1021/jp306175b

[103] P. Ngene, S.F.H. Lambregts, D. Blanchard, T. Vegge, M. Sharma, H. Hagemann, P.E. De Jongh, The influence of silica surface groups on the Li-ion conductivity of $LiBH_4$/SiO_2 nanocomposites, Phys. Chem. Chem. Phys. 21 (2019) 22456–22466, https://doi.org/10.1039/c9cp04235k

[104] S.F.H. Lambregts, E.R.H. Van Eck, Suwarno, P. Ngene, P.E. De Jongh, A.P.M. Kentgens, Phase behavior and ion dynamics of nanoconfined $LiBH_4$ in silica, J. Phys. Chem. C. 123 (2019) 25559–25569, https://doi.org/10.1021/acs.jpcc.9b06477

[105] Suwarno, P. Ngene, A. Nale, T.M. Eggenhuisen, M. Oschatz, J.P. Embs, A. Remhof, P.E. De Jongh, Confinement effects for lithium borohydride: comparing silica and carbon scaffolds, J. Phys. Chem. C. 121 (2017) 4197–4205, https://doi.org/10.1021/acs.jpcc.6b13094

[106] Y.S. Choi, Y.S. Lee, K.H. Oh, Y.W. Cho, Interface-enhanced Li ion conduction in a $LiBH_4$-SiO_2 solid electrolyte, Phys. Chem. Chem. Phys. 18 (2016) 22540–22547, https://doi.org/10.1039/c6cp03563a

[107] J. Lefevr, L. Cervini, J.M. Griffin, D. Blanchard, Lithium conductivity and ions dynamics in $LiBH_4$/SiO_2 solid electrolytes studied by solid-state NMR and quasi-elastic neutron scattering and applied in lithium-sulfur batteries, J. Phys. Chem. C. 122 (2018) 15264–15275, https://doi.org/10.1021/acs.jpcc.8b01507

[108] Y. Dou, H.A. Hansen, S.M. Xu, D. Blanchard, Layered double hydroxides as advanced tracks to promote ionic conductivity in metal borohydride, Mater. Chem. Front. 5 (2021) 4989–4996, https://doi.org/10.1039/d1qm00059d

[109] Z. Liu, M. Xiang, Y. Zhang, H. Shao, Y. Zhu, X. Guo, L. Li, H. Wang, W. Liu, Lithium migration pathways at the composite interface of $LiBH_4$ and two-dimensional MoS_2 enabling superior ionic conductivity at room temperature, Phys. Chem. Chem. Phys. 22 (2020) 4096–4105, https://doi.org/10.1039/c9cp06090a

[110] Y. Yan, D. Rentsch, C. Battaglia, A. Remhof, Synthesis, stability and Li-ion mobility of nanoconfined $Li_2B_{12}H_{12}$, Dalt. Trans. 46 (2017) 12434–12437, https://doi.org/10.1039/C7DT02946B

[111] M.S. Andersson, V. Stavila, A.V. Skripov, M. Dimitrievska, M.T. Psurek, J.B. Leão, O.A. Babanova, R.V. Skoryunov, A.V. Soloninin, M. Karlsson, T.J. Udovic, Promoting persistent superionic conductivity in sodium monocarba- closo -dodecaborate $NaCB_{11}H_{12}$ via confinement within nanoporous silica, J. Phys. Chem. C. 125 (2021) 16689–16699, https://doi.org/10.1021/acs.jpcc.1c03589

[112] F. Lu, Y. Pang, M. Zhu, F. Han, J. Yang, F. Fang, D. Sun, S. Zheng, C. Wang, A high-performance Li–B–H electrolyte for all-solid-state Li batteries, Adv. Funct. Mater. 29 (2019) 1–7, https://doi.org/10.1002/adfm.201809219

[113] R. Zettl, L. de Kort, M. Gombotz, H.M.R. Wilkening, P.E. de Jongh, P. Ngene, Combined effects of anion substitution and nanoconfinement on the ionic conductivity of Li-based complex hydrides, J. Phys. Chem. C. 124 (2020) 2806–2816, https://doi.org/10.1021/acs.jpcc.9b10607

[114] R. Zettl, M. Gombotz, D. Clarkson, S.G. Greenbaum, P. Ngene, P.E. de Jongh, H.M.R. Wilkening, Li-ion diffusion in nanoconfined $LiBH_4$-LiI/Al_2O_3: from 2D bulk transport to 3D long-range interfacial dynamics, ACS Appl. Mater. Interfaces 12 (2020) 38570–38583, https://doi.org/10.1021/acsami.0c10361

[115] S. Breuer, V. Pregartner, S. Lunghammer, H.M.R. Wilkening, Dispersed solid conductors: fast interfacial Li-Ion dynamics in nanostructured LiF and LiF γ-Al_2O_3 composites, J. Phys. Chem. C. 123 (2019) 5222–5230, https://doi.org/10.1021/acs.jpcc.8b10978

[116] R. Zettl, K. Hogrefe, B. Gadermaier, I. Hanzu, P. Ngene, P.E. De Jongh, H.M.R. Wilkening, Conductor-insulator interfaces in solid electrolytes: a design strategy to enhance Li-Ion dynamics in nanoconfined $LiBH_4$/Al_2O_3, J. Phys. Chem. C. 125 (2021) 15052–15060, https://doi.org/10.1021/acs.jpcc.1c03789

[117] G.P. Meisner, M.L. Scullin, M.P. Balogh, F.E. Pinkerton, M.S. Meyer, Hydrogen release from mixtures of lithium borohydride and lithium amide: a phase diagram study, J. Phys. Chem. B. 110 (2006) 4186–4192, https://doi.org/10.1021/jp056019b

[118] T. Noritake, M. Aoki, S. Towata, A. Ninomiya, Y. Nakamori, S. Orimo, Crystal structure analysis of novel complex hydrides formed by the combination of $LiBH_4$ and $LiNH_2$, Appl. Phys. A Mater. Sci. Process. 83 (2006) 277–279, https://doi.org/10.1007/s00339-006-3500-9

[119] M. Matsuo, A. Remhof, P. Martelli, R. Caputo, M. Ernst, Y. Miura, T. Sato, H. Oguchi, H. Maekawa, H. Takamura, A. Borgschulte, A. Züttel, S.I. Orimo, Complex hydrides with $(BH_4)^-$ and $(NH_2)^-$ anions as new lithium fast-ion conductors, J. Am. Chem. Soc. 131 (2009) 16389–16391, https://doi.org/10.1021/ja907249p

[120] Q. Yang, F. Lu, Y. Liu, Y. Zhang, X. Wang, Y. Pang, S. Zheng, $Li_2(BH_4)(NH_2)$ nanoconfined in SBA-15 as solid-state electrolyte for lithium batteries, Nanomaterials 11 (2021) 946, https://doi.org/10.3390/nano11040946

[121] Y. Yan, J.B. Grinderslev, Y.S. Lee, M. Jørgensen, Y.W. Cho, R. Černý, T.R. Jensen, Ammonia-assisted fast Li-ion conductivity in a new hemiammine lithium borohydride, $LiBH_4.1/2NH_3$, Chem. Commun. 56 (2020) 3971–3974, https://doi.org/10.1039/c9cc09990e

[122] W. Zhao, R. Zhang, H. Li, Y. Zhang, Y. Wang, C. Wu, Y. Yan, Y. Chen, Li-Ion conductivity enhancement of $LiBH_4$·xNH_3 with in situ formed Li2O nanoparticles, ACS Appl. Mater. Interfaces 13 (2021) 31635–31641, https://doi.org/10.1021/acsami.1c06164

[123] M. Latroche, D. Blanchard, F. Cuevas, A. El Kharbachi, B.C. Hauback, T.R. Jensen, P.E. de Jongh, S. Kim, N.S. Nazer, P. Ngene, S. ichi Orimo, D.B. Ravnsbæk, V.A. Yartys, Full-cell hydride-based solid-state Li batteries for energy storage, Int. J. Hydrog. Energy 44 (2019) 7875–7887, https://doi.org/10.1016/j.ijhydene.2018.12.200

[124] A. Unemoto, T. Ikeshoji, S. Yasaku, M. Matsuo, V. Stavila, T.J. Udovic, S.I. Orimo, Stable interface formation between TiS_2 and $LiBH_4$ in bulk-type all-solid-state lithium batteries, Chem. Mater. 27 (2015) 5407–5416, https://doi.org/10.1021/acs.chemmater.5b02110

[125] S. Das, P. Ngene, P. Norby, T. Vegge, P.E. de Jongh, D. Blanchard, All-solid-state lithium-sulfur battery based on a nanoconfined $LiBH_4$ electrolyte, J. Electrochem. Soc. 163 (2016) A2029–A2034, https://doi.org/10.1149/2.0771609jes

[126] V. Gulino, M. Brighi, F. Murgia, P. Ngene, P. de Jongh, R. Černý, M. Baricco, Room-temperature solid-state lithium-ion battery using a $LiBH_4$ –MgO composite electrolyte, ACS Appl. Energy Mater. 4 (2021) 1228–1236, https://doi.org/10.1021/acsaem.0c02525

[127] R. Asakura, D. Reber, L. Duchêne, S. Payandeh, A. Remhof, H. Hagemann, C. Battaglia, 4 V room-temperature all-solid-state sodium battery enabled by a passivating cathode/hydroborate solid electrolyte interface, Energy Environ. Sci. 13 (2020) 5048–5058, https://doi.org/10.1039/d0ee01569e

[128] J. Lamb, J.A. Jeevarajan, New developments in battery safety for large-scale systems, MRS Bull. 46 (2021) 395–401, https://doi.org/10.1557/s43577-021-00098-0

[129] W.S. Tang, K. Yoshida, A.V. Soloninin, R.V. Skoryunov, O.A. Babanova, A.V. Skripov, M. Dimitrievska, V. Stavila, S.I. Orimo, T.J. Udovic, Stabilizing Superionic-conducting structures via mixed-anion solid solutions of monocarba-closo-borate salts, ACS Energy Lett. 1 (2016) 659–664, https://doi.org/10.1021/acsenergylett.6b00310